ChemPubSoc Europe
DOI: 10.1002/cptc.201900034
CHEMPHOTOCHEM Reviews

Special Issue

Photoresponsive Chiral Dopants: Light-Driven Helicity Manipulation in Cholesteric Liquid Crystals for Optical and Mechanical Functions

Yuna Kim*[a] and Nobuyuki Tamaoki*[a]

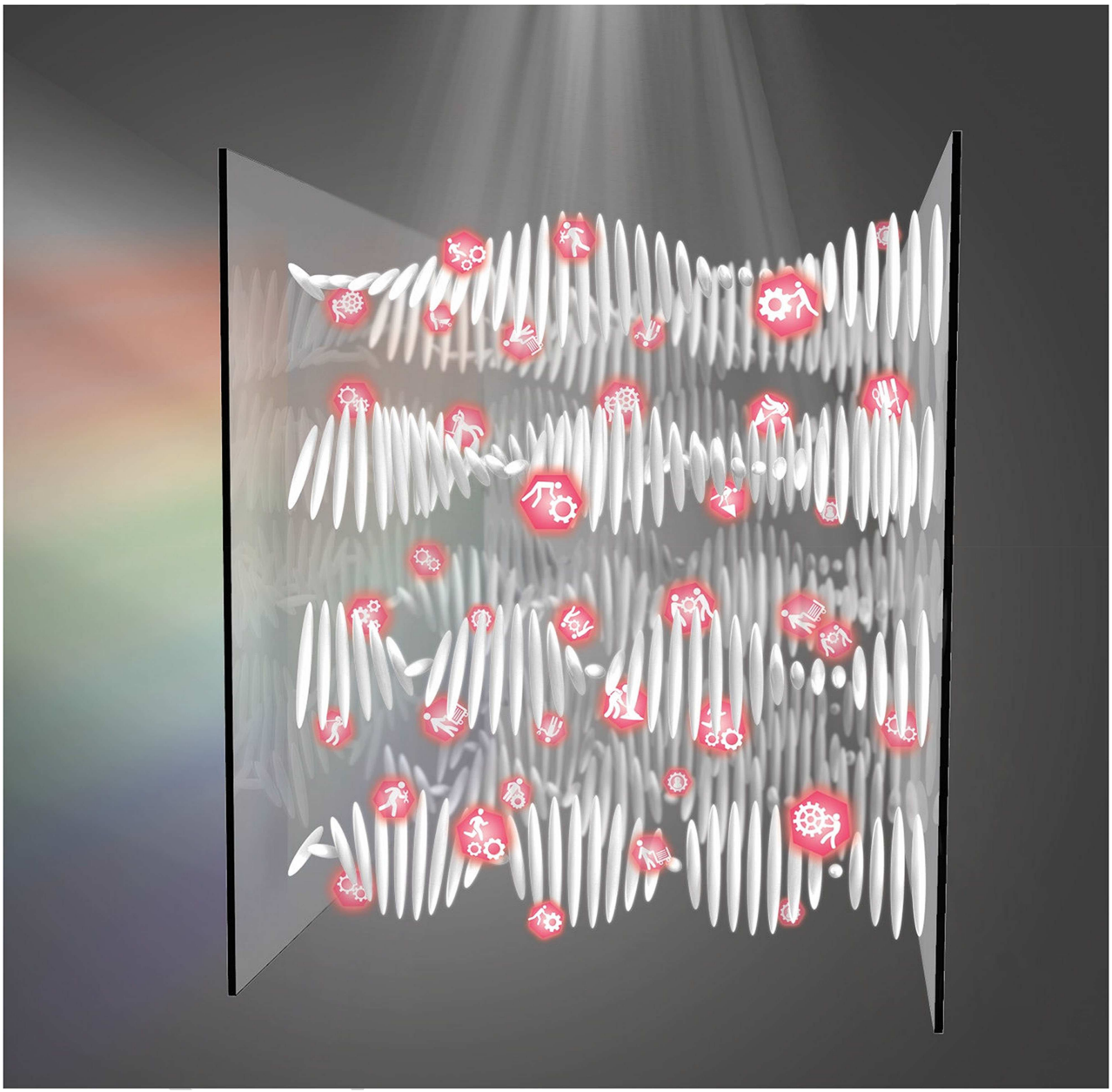

© 2019 Wiley-VCH Verlag GmbH & Co. KGaA, Weinheim

This Review focuses on recent advancements regarding the design of photoisomerizable chiral dopants which can switch the helical orientation in cholesteric liquid crystals upon light stimuli. Chiral dopants exhibiting conformational change in response to an external stimulus can provide dynamic control of the cholesteric pitch. Development of such responsive systems has been attempted since the 1970s. However, major advances on efficient chiral dopants exhibiting either high helical twisting power or large photoswitching have been achieved only in recent years. This Review covers photo-responsive low molecular weight cholesteric liquid crystal systems based on chiral dopants capable of photochemically "switching power to twist" surrounding liquid crystalline host molecules, "inverting" their handedness or even "inducing" helical organization from the racemic nematic phase.

1. Introduction

Molecular chirality has a conformational and configurational origin, but supramolecular level chirality originates from the organization of molecules in a long-range orientational orders forming chiral superstructure.[1] The supramolecular level chirality can be usually obtained by transmission of chiral information of the chiral molecule to the host medium via anisotropic intermolecular interactions. In comparison to crystalline phases, liquid crystalline phases have both elastic property and orientational order with a relatively lower degree of organization. Accordingly, liquid crystals (LCs) have shown their capabilities as host medium: transfer chiral guest information to the entire system through amplification.[2] At the low molecular weight (LMW) supramolecular level, helical organization typically takes place in chiral smectic and chiral nematic (cholesteric, N*) liquid crystals.[3] The director of these LCs rotates in a helical manner with a pitch (*P*) which is the distance along the helical axis on a completion of a full turn of the molecules. A cholesteric liquid crystal (CLC) has a specific handedness: positive handedness denotes a right-handed helix, whereas a negative handedness represents a left-handed helix. The periodic helical superstructures can selectively reflect the circularly polarized light (CPL) of a certain wavelength which matches its helical pitch length (Scheme 1).

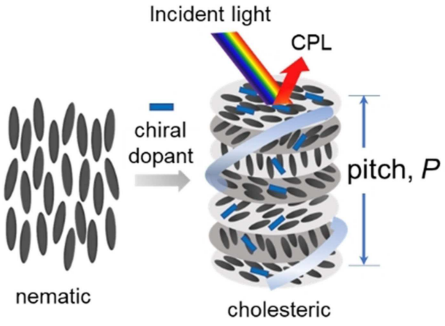

Scheme 1. Schematic illustration of transition from the nematic to the cholesteric phase by doping with a chiral dopant.

To mimic the homochirality of nature and to create smart supramolecular systems, adopting external stimuli has been an important issue in terms of generation and control of the asymmetry at various scales.[4] Since the CLC is based on nematic LC which has the highest degree of freedom among the LC phases, its molecular organization is highly responsive to various external stimuli such as temperature,[5] electric field,[6] pressure,[7] dopants,[8] and light.[4,9] Among the possible external stimuli, light has tunability of its intensity, wavelength, exposure area, remote control, and polarizability- ambient, linear, circular polarization- which allows versatile control of the mesomorphic reorganization. In 1971, Sackmann reported that the optical reflection band of CLCs shifts reversibly based on the photoisomerization of the doped azobenzene molecules.[10] This demonstration has accelerated the utilization of photochemistry of molecular switches (dopants) for light-driven optical applications of CLCs. When a photochromic dopant has a chiral element, not only an enantiomeric imbalance of achiral (racemic) LCs but also photo-triggering/transmittance of its chiral information to the host LC medium can be achieved (Scheme 2).[11] The ability of a photochromic chiral dopant to induce a helical structure in an achiral nematic LC can be described as a parameter, helical twisting power, HTP (β), as expressed in Equation (1):

$$\beta = 1/P \cdot C \cdot ee \quad (1)$$

in which *C* and *ee* are the concentration and photoinduced enantiomeric excess of the chiral dopant, respectively, and *P* is the pitch length.[11] Accordingly, a photoisomerizable chiral dopant with a strong chirality transfer property exhibits a high HTP value associated with a short pitch length showing reflection band in short wavelength, whereas a decrease of HTP results in elongation of pitch length and a redshift of its reflection band. It is noteworthy that achieving high initial HTP value and its large photoinduced variation ($\Delta\beta$) is advantageous for the quantity necessary to induce and modulate the cholesteric phase (low doping concentration). It contributes to the reflection color tunability over a wide range of wavelengths. Typically, the high dopant concentration is likely to show coloration in CLC, phase separation or alternation to undesired physical properties such as a transition to the isotropic phase.[12]

[a] *Dr. Y. Kim, Prof. N. Tamaoki*
Research Institute for Electronic Science
Hokkaido University
N-20, W-10, Kita-Ku, Sapporo, Hokkaido, 001-0020 (JAPAN)
E-mail: ykim@es.hokudai.ac.jp
tamaoki@es.hokudai.ac.jp

An invited contribution to a Special Issue on Photoresponsive Molecular Switches and Machines

© 2019 Wiley-VCH Verlag GmbH & Co. KGaA, Weinheim

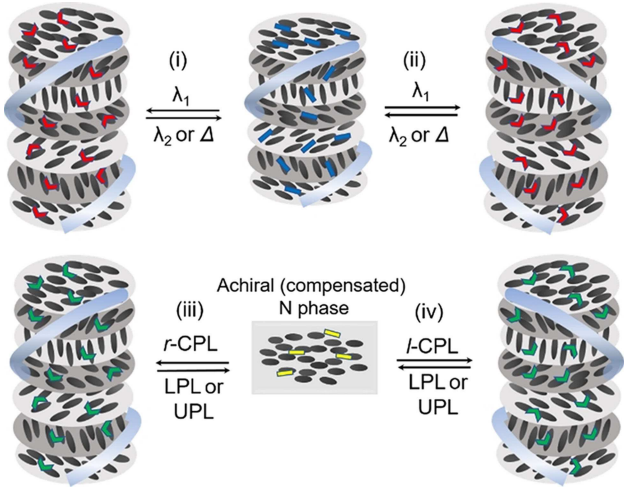

Scheme 2. Several types of reversible tuning of helical superstructure by the photochemical reaction of chiral dopants: (i) helical pitch elongation and shortening with the same handedness or (ii) accompanying handedness inversion upon unpolarized light irradiation of two different wavelengths, λ_1 and λ_2 (*e.g.* UV or visible light), or heat. Photochemical chirality induction in an achiral nematic phase doped with a racemic dopant upon circularly polarized light (CPL) irradiation of (iii) a right-handed system (***r***-CPL), or (iv) a left-handed system (***l***-CPL) and its racemization upon linearly polarized light (LPL) or unpolarized light (UPL) irradiation.

In addition to the relative contrast in HTP values (Scheme 2, i), some configurational phototunability of CLC can also provide handedness invertible helical reorganization (Scheme 2, ii). At the helix inversion point in between the cholesteric phases with opposite handedness, the net HTP value becomes zero because of the presence of equal amounts of the isomers with opposite signs.[4] Accordingly, the pitch reaches an infinite value which results in the formation of an achiral nematic phase which can also be referred to as a racemic mixture of left- and right-handed CLCs.[4,13] Also, based on the partial photoresolution of photoresponsive chiral dopant, the induction of cholesteric phase from racemic phase can be achieved in which its HTP is related to the photoinduced enantiomeric excess (Scheme 2, iii and iv).

In recent years, numerous photoresponsive CLC systems have been elaborated enabling diverse modulation of HTP and resultant cholesteric pitch and handedness described above. Tunable chirality coupled with photoisomerizable moiety[11b]

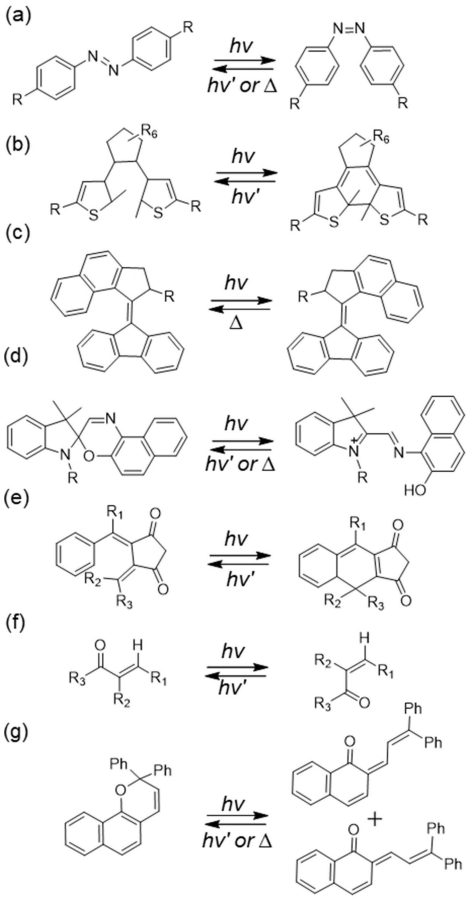

Scheme 3. Molecular structures and reversible photoisomerization of molecular switches which are generally utilized as photoresponsive dopants for LCs: azobenzene (a), diarylethene (b), overcrowded alkene (c), spirooxazine (d), fulgide (e), α,β-unsaturated ketone (f) and naphthopyran (g).

(Scheme 3) such as azobenzene (a),[14] diarylethene (b),[15] overcrowded alkene (c),[16] spirooxazine (d),[17] fulgide (e),[18] unsaturated ketone (f)[19] and naphthopyran (g)[20] leads to CLCs exhibiting photoresponsive chiroptical functions with amplified responses. Their genuine applications include advanced reflective displays without any color filter or polarizer,[21] reflectors,[22] tunable lasers[23] and diffraction beam steering.[24] Besides, light-driven molecular motor applications and actuators executing mechanical functions have been demonstrated based on

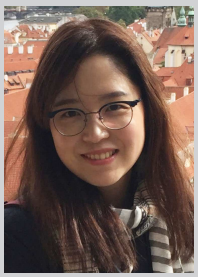

Yuna Kim received her B.S. (2005), M.S. (2007) and Ph.D. (2011) in chemical engineering from Yonsei University, Korea on the study of electrochromic and electrofluorochromic materials. She worked as a postdoctoral researcher at the Active Polymer Centre for Pattern Integration (2011). She joined the faculty at Hokkaido University in 2011. She is currently an associate professor at the Research Institute for Electronic Science, Hokkaido University. Her research interests include the development of external stimuli-responsive various chromogenic materials with novel functions.

Nobuyuki Tamaoki obtained his Ph.D degree from Chiba University in Japan. After working as a researcher, a senior researcher and a group leader at Japanese government's research institutes including the National Institute of Advanced Industrial Science and Technology, he moved to Hokkaido University as a full professor in 2008. Currently he is also a director of the Green Nanotechnology Center of the University. His research interests include photochemistry, stereochemistry, organic synthesis, molecular switches and motors and self-assembled molecular systems.

© 2019 Wiley-VCH Verlag GmbH & Co. KGaA, Weinheim

dynamic superstructure switching of CLCs in micro/macroscales.[25]

In this review, we report on the recent development harnessing supramolecular chiral assemblies based on chiral photochromic switches in LMW achiral LCs. Single molecular chirality propagation to meso/macroscopic level and its versatile photocontrol is introduced and the promising applications for advanced optical and mechanical systems are summarized.

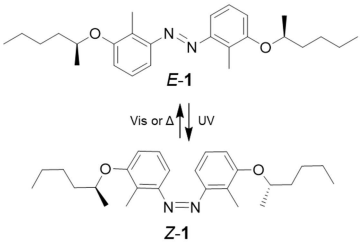

Figure 1. 3,3-Disubstituted chiral azobenzene dopant (**1**) showing high compatibility with LCs in its *cis*-form.

2. Photoresponsive Chiral Dopants for Cholesteric Liquid Crystals

2.1. Chiral Azobenzenes

Azobenzene undergoes *trans* (E)-*cis* (Z) isomerization (Scheme 3a). Especially in the study of the structure-property relation in cholesteric phase, it appears to be an appealing phototrigger because of its simple molecular structure and decent photo fatigue resistance.[9a] Besides, the geometrical changes resulting from photoisomerization of rod-shaped *trans* form to bent *cis* from affect the large extent of the twisting ability of chiral moieties. Considerable progress on high HTP from point, axially or planar chiral azobenzene dopants is covered in this section.

2.1.1. Point Chiral Azobenzenes

Point chiral auxiliaries such as cholesterol, isosorbide, menthol and alkyl spacer with chirality centers are commonly utilized to various photochromic dopants. These point chiral substituents are rather weak helical inducers compared with those of axial or planar moieties. Thus, herein, we focus to introduce some unique aspects achieved from point chiral azobenzene dopants. In general, rodlike *trans*-isomers show higher HTP than that of bent *cis*-isomers in cholesteric phase because of higher compatibility of trans-form with nematic LC host molecules.[14] Exceptions are rare showing higher cholesteric induction in cis-form, but some azobenzene dopants possessing central chirality fall into this category though they have intrinsically low HTP values compared with chiral azobenzenes bearing atropisomeric moieties.

The first dopant demonstrated by the Ichimura group[14] contains azobenzene with spacer substitutions at the 3,3′-positions and at the *ortho*-position (**1**). The *cis* isomer showed higher HTPs (8.9 μm^{-1} (mol%) in nematic DON-103) which has more elongated rodlike conformation relative to its *trans* isomer (3.1 μm^{-1} (mol%) in DON-103) (Figure 1).

Later, the Kurihara group reported that the molecular aspect ratio (molecular length divided by diameter) can influence the intermolecular interactions between host LCs and chiral dopants. *Meta*-substituted azobenzene with chiral isosorbide moiety (**2**; Figure 2) of a higher molecular aspect ratio in the *cis*-rich state exhibited a higher HTP ($79.4\times 10^8\ m^{-1}\ mol^{-1}\ gE44$) than that in the *trans* state ($15.6\times 10^8\ m^{-1}\ mol^{-1}\ gE44$).[21b]

Recently, our group observed the HTP increment in the *cis*-rich state of a *para*-substitution azobenzene (**3**) which is more generalized structure compared with the two cases mentioned above. The cooperative effect of chirality and photoisomerization was exploited from cholesterol and azobenzene units, respectively, in the form of two mesogens connected by means of a flexible linker. A rigid and long molecular shape can stabilize parallel molecular stacking by anisotropic intermolecular interactions through van der Waals forces. Therefore, it assists the localized formation of smectic-like cybotactic domains in a helical superstructure (Figure 3b). This elongated cybotactic cluster containing *trans*-form dopants is likely to disrupt the helical molecular orientation in the CLCs resulting in lower HTP: its reversible decay (higher HTP, 0.99 μm^{-1} in nematic JC-1041XX) and reassembly (lower HTP, 0.66 μm^{-1} in JC-1041XX) was evidenced by *in-situ* X-ray diffraction pattern upon sequential irradiation of UV and visible light, respectively (Figure 3c). Not only the photoisomerization of the azobenzene units, also the odd/even parity of the linkers in the asymmetric dimers largely affected the transition behaviour of the cybotactic domains. **3** (n = 3) exhibited the highest initial HTP of 2.37 μm^{-1} in nematic 5CB but the smallest photoswitching which indicates the unlikely obtainable smectic clusters due to its inherent bent shape in *trans*-form.

Meanwhile, the large rotational reorganization of the cholesteric helix and HTP switching ($\Delta\beta/\beta_{ini}$ up to 50%) by the modulation of the cybotactic clusters encouraged us to photocontrol the macroscopic rotational motion of microsized glass rods floating on the surface of a CLC film showing a polygonal fingerprint texture (Figure 3d). **3** (n = 2) doped CLC (5 wt% in JC-1041XX) showed the maximum rotational angle under irradiation with both UV (a clockwise rotational angle of 430°) and visible (a counterclockwise rotational angle of 370°) light

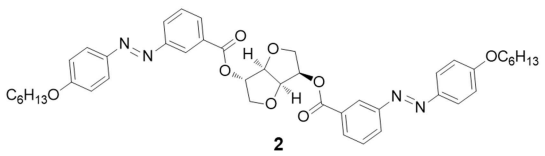

Figure 2. *Meta*-substituted chiral azobenzene with isosorbide moiety (**2**) showing HTP increment in its *cis*-rich state.

© 2019 Wiley-VCH Verlag GmbH & Co. KGaA, Weinheim

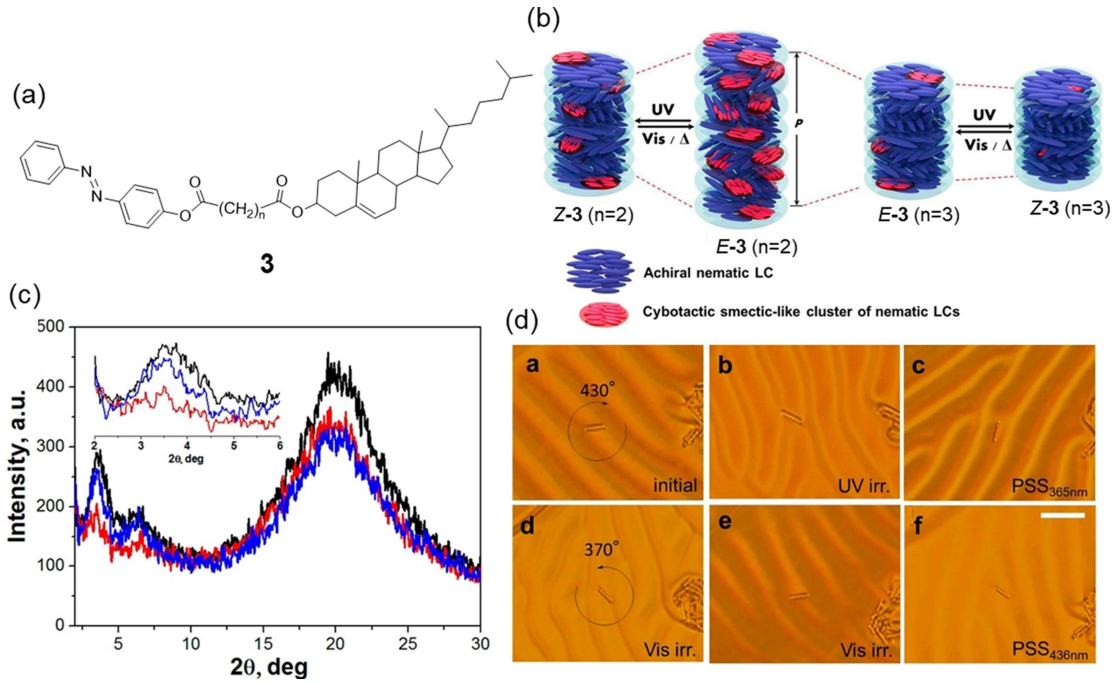

Figure 3. (a) Asymmetric dimeric chiral azobenzenes substituted with cholesterol moiety (**3**). (b) Schematic representation of cybotactic smectic clusters formed in CLC and its different photoinduced fluctuation behavior with even (n = 2)-/odd (n = 3)-numbered methylene linkers of **3**. (c) Intensity profiles in the XRD patterns of **3** (n = 2), doping concentration of 0.1 wt % in 5CB, before photoirradiation (initial, black line) and after irradiation with UV (red line) and visible (blue line) light at each photostationary state (PSS). Inset: Magnified XRD patterns featuring smectic fluctuation region. (d) Rotational motion of a microsize glass rod on the surface of a CLC film (5 wt% of **3** in JC-1041XX) starting from a) the initial state to c) $PSS_{365\ nm}$, d) followed by irradiation with visible light to f) $PSS_{436\ nm}$. Images were taken sequentially. White scale bar: 50 μm. Reproduced from ref.[26] with permission. Copyright 2016 American Chemical Society.

over one full cycle. It is noteworthy that such a large reorganization can be achieved from a small HTP.

A compensated nematic phase can be defined as an achiral phase originating from a racemic mixture of equal amounts of chiral dopants with opposite handedness in a host nematic liquid crystal. This phenomenon is generally detected during the switching between two cholesteric phases which have opposite twist sense. Kurihara et al.[25b,27] reported a compensated nematic phase in the nonirradiated initial state. The reversible switching of the racemic-cholesteric phase was achieved by *trans-cis* photoisomerization through UV and visible light irradiation. In addition, the rotational and translational movement of the microscale object was subjected by light. Chiral azobenzene compound (**4**), photo-inactive chiral dopant (**5**) and nematic E44 were utilized for cholesteric or compensated nematic LCs. The optical isomers determine the rotation direction as shown in Figure 4b. Also, translational motion of the object was observed when a racemic mixture of **4** was introduced (Figure 4c). The spatially controlled irradiation of Ar^+ laser and a diode UV laser could provide more facile and precise manipulation of the object in a translational motion.[25b]

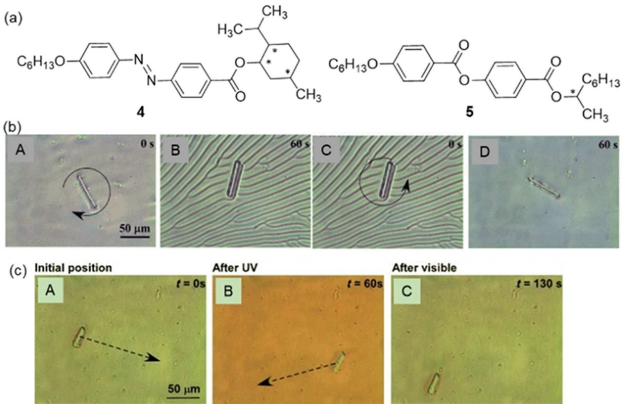

Figure 4. (a) Molecular structures of chiral dopants (**4** and **5**). Optical micrographs of rotational (b) and translational (c) glass rod movement on the surface of compensated nematic LC film upon light irradiation: (b) doped with D-**4** and **5** (S-811) in nematic E44 showing clockwise rotation (A–B) upon UV light ($\lambda = 365$ nm) irradiation and counterclockwise rotation (C–D) by visible light ($\lambda = 436$ nm) irradiation; (c) doped with racemic **4** (6 wt% in E44) showing a rodlike movement from the initial position (A) to the right-hand side towards the irradiation position and to the left-hand side in the opposite direction upon UV ($\lambda = 365$ nm) and visible ($\lambda = 436$ nm) light irradiation, respectively. Reproduced from Ref. [25b] with permission. Copyright 2011 Wiley-VCH.

2.1.2. Axially Chiral Azobenzenes

One of the most extensively studied classes of photoresponsive chiral dopants would contain binaphthyl moieties possessing inherent axial chirality. The binaphthyl unit has restricted freedom of internal rotation along the carbon-carbon bond between its 1 and 1′ positions. The dihedral angle (θ) between the two naphthyl rings- *cisoid* ($\theta < 90°$) or *transoid* ($\theta > 90°$) geometry- determines the helicity of the binaphthyl derivative.[28] Thus, it is known as a

© 2019 Wiley-VCH Verlag GmbH & Co. KGaA, Weinheim

feasible unit to control both helical sense and twist strength of the CLC. Ever since the first demonstration on axially chiral azobenzene (**6**)[29] bearing two azo moieties to the 2,2′ positions of binaphthyl, lots of CLC systems based on binaphthyl azoarene dopants have been developed.[30] Those axially chiral azobenzenes could maintain the C_2 symmetry of binaphthyl and gave strong responses to the stereochemical variations and photochemical isomerization. (*R*)-**6** exhibited high initial HTPs of $+148\ \mu m^{-1}$ (mol %) in E7,[29,30a] and extending mesogen unit with phenyl moiety (**7**) elevated its initial HTP value to $+201\ \mu m^{-1}$ (mol%) in phase 1052 accompanying its large switching to $+106\ \mu m^{-1}$ (mol%) at UV light irradiation induced photostationary state (PSS_{UV}).[30a] Compound **8**[30b] substituted with long alkoxy spacers exhibited decent HTP values ranging 57 μm^{-1} (158 μm^{-1} (mol%)). Besides, optically addressed reflection color images could be demonstrated with a high-resolution and gray scale based on CLC containing 6% of **8** doped in E7 (Figure 5b). Meanwhile, substituting binaphthyl unit

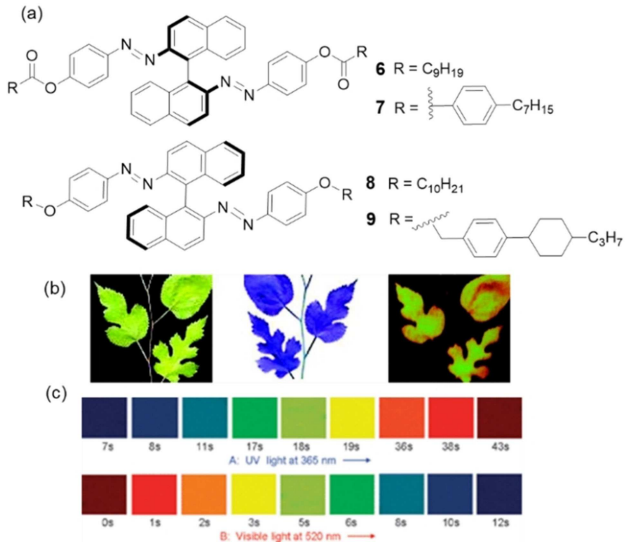
(a)
6 R = C9H19
7 R = C7H15
8 R = C10H21
9 R = C3H7
(b)
(c)
7s 8s 11s 17s 18s 19s 36s 38s 43s
A: UV light at 365 nm
0s 1s 2s 3s 5s 6s 8s 10s 12s
B: Visible light at 520 nm

Figure 5. (a) Axially chiral azobenzene dopants (**6**-**9**). (b) Regular photograph of the original digital image (left), its negative photo mask image (middle), and image optically recorded on the CLC display cell based on **8** doped in E7 (right). Reproduced from ref.[30b] with permission. Copyright 2007 American Chemical Society. (b) Reflection colors obtained from 6.5 wt% of **9** in E7 (5 μm thick planar cell). A: upon irradiation at 365 nm (5.0 mW cm^{-2}); B: upon irradiation at 520 nm (1.5 mW cm^{-2}) with different times. Reproduced from Ref. [30c] with permission. Copyright 2010 The Royal Society of Chemistry.

with two rodlike mesogens via methyleneoxy linkers (**9**)[30c] led to both good solubility in LC host (E7) and high HTP of 90 μm^{-1} (304 μm^{-1}(mol%)). It is attributable to the molecular structure of the cyclohexylphenyl moieties resembling the hosts. Subsequent UV and visible light irradiation resulted in the large HTP switching to 26 μm^{-1} (at PSS_{UV}) and 58 μm^{-1} (at PSS_{VIS}), respectively. **9** enabled the reversible phototuning of the various reflection colors including RGB at 6.5 wt% in E7 by UV and visible light irradiation as shown in Figure 5c.

Besides, introducing additional chiral moieties to the two ends of binaphthyl azobenzenes has been attempted. Axially chiral azoarene compounds containing binaphthyls of both the same and opposite chiral configurations (**10**) are shown in Figure 6a.[31] Among the four kinds of chiral handedness and spacer length

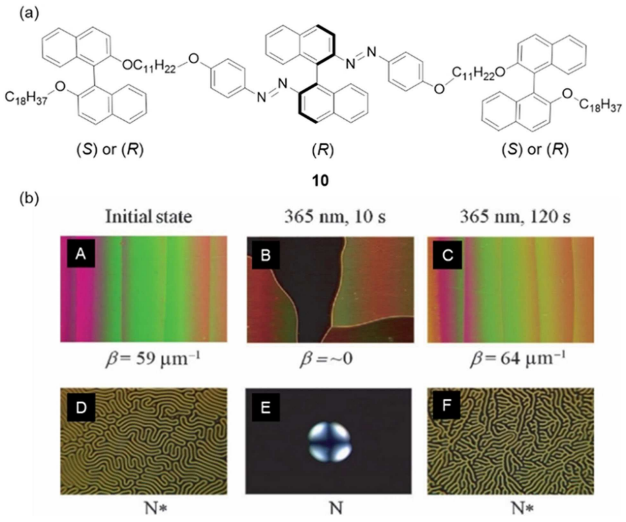

Figure 6. (a) Chemical structure of dopants **10**. (b) Crossed polarizing microscopic images of 0.27 mol% (*S,R,S*)-**10** in 5CB showing handedness inversion observed in a wedge cell (A–C) and homeotropic cell (D–F) from right-handed (A,D) to left-handed cholesteric phase (C,F) via a transient achiral nematic phase (B,E). Reproduced from Ref. [31] with permission. Copyright 2013 Wiley-VCH.

combinations, the highest initial HTP was obtained as 242 μm^{-1} (mol%) from (*R,R,R*) derivative in 5CB. Interestingly, the handedness inversion was observed in CLCs doped **10** with opposite chiral configurations (*S,R,S*) upon UV light irradiation. It showed the chiral nematic and racemic nematic phases, subsequently the recovery of original handedness and HTP (up to 90%) at photostationary state (PSS_{VIS}) (Figure 6b). In contrast, **10** with the same chiral configurations (*R,R,R*) showed no inversion of its handedness. Thus, providing chiral conflict to the molecular level possibly induces a shift of the equilibrium between opposite chiral configurations in a single chiral switch.

Meanwhile, axially chiral azobenzenes introduced with noncovalent interactions such as hydrogen bonding or halogen bonding have been reported. It offered a versatile tool to assemble readily available building blocks with photoresponsive chiral molecular switches (Figure 7). Fu et al. have investigated a binaphthyl azobenzene incorporated with additional chiral units through hydrogen bond (**11** in Figure 7a).[32a] In order to form H-bonded chiral switches, the binaphthyl azobenzene unit was introduced as a proton acceptor and binaphthyl acids with opposite chiral configurations were used as proton donors. Figure 7b shows a phase transition from N* to N accompanying the helical inversion and HTP switching upon light irradiation. The terminal alkyl chain length of proton donors influenced the HTP as well as helix inversion characteristics of CLCs. The HTP values measured for compound **11** are relatively smaller than those measured for **10**, however the switching ratio reaches over 800% (Table 1).

Recently, Li et al.[32b] utilized halogen bonding to an axially chiral azoarene (**12** in Figure 7a). The halogen bond in **12** was

© 2019 Wiley-VCH Verlag GmbH & Co. KGaA, Weinheim

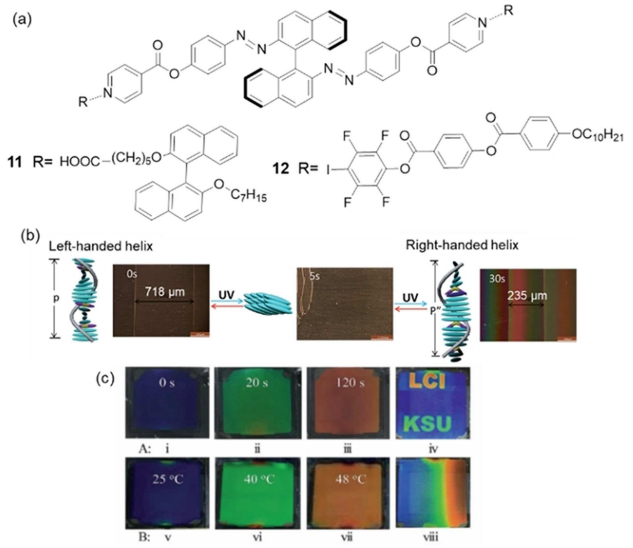

Figure 7. (a) Noncovalently bonded chiral azobenzene dopants (**11** and **12**). (b) Polarizing optical microscope (POM) images of CLCs containing (*R*,*S*,*R*)-**11** (1.0 wt%) in a wedge cell between the *trans* state (left image) and PSS_{UV} (right image) by irradiation of UV ($\lambda = 365$ nm, 2 mW cm^{-2}) at 25 °C. Schematics along the corresponding reversible helical inversion between N*–N–N* phase transition sequence with opposite handedness. Reproduced from Ref. [32a] with permission. Copyright 2015 The Royal Society of Chemistry. (c) Real cell images of a planar cell filled with (*S*)-**12** (2.8 mol%) in E7: (A) upon 365 nm UV irradiation and (B) heating; RGB color in a single cell obtained by (iv) photopatterning and (viii) temperature gradient. Reproduced from Ref. [32b] with permission. Copyright 2018 Wiley-VCH.

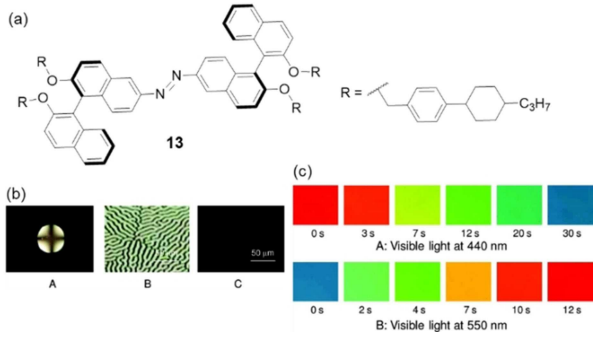

Figure 8. (a) Molecular structure of **13**. (b) Crossed-polarized textures of 1.5 wt% of (*S*,*S*)-**13** in E7 in a homeotropically aligned cell at RT: (A) initial state with conoscopic texture; (B) after irradiation at 440 nm for 30 s; (C) followed by irradiation at 550 nm for 15 s. (c) Polarized reflective mode microscope images of 22.7 wt% (*S*,*S*)-**13** in E7 in a planar cell: (A) during the irradiation at 440 nm; (B) reverse process upon irradiation at 550 nm. Reproduced from ref.[33] with permission. Copyright 2012 American Chemical Society.

formed between pyridyl-substituted binaphthyl azobenzene moiety (halogen-bond acceptor) and the 4-iodotetrafluorophenyl moiety (halogen-bond donor). Initial HTP of **12** was 136 μm^{-1} (mol%) and it decreased to 97 μm^{-1} (mol%) upon UV light irradiation. While, HTP of the photoresponsive chiral halogen-bond acceptor itself was 99 μm^{-1} (mol%) which is lower than that of **12**. With a CLC film containing 2.8 mol% of **12** in E7, the primary RGB colors could be obtained both photochemically and thermally (Figure 7c).

In addition, visible light sensitive chiral azobenzenes have been developed by tailoring either photoresponsive units or mesogen units. One approach is the π-conjugation extension of the aromatic groups which are linked to the azobenzene moiety (**13** in Figure 8a).[33] A noticeable feature of this system is that initial HTP of **13** increased upon 440 nm light irradiation from 52 to 89 μm^{-1} (mol%) and its initial recovered close the HTP value of 58 μm^{-1} (mol%) upon 550 nm light irradiation. It is quite rare case because HTP value usually decreases upon transition to *cis*-rich state, but its mechanism is unclear. The authors mentioned that the increase in HTP might be due to the change in the dihedral angle of the binaphthyl groups. At a low doping concentration of 1.5 wt%, photochemical cholesteric phase induction from achiral nematic phase was obtainable upon 440 nm light irradiation (Figure 8b). Moreover, high doping level of 22.7 wt% (*S*,*S*)-**13** in E7 resulted in reversible RGB phototuning process upon 440 nm and 550 nm light irradiation (Figure 8c).

Other approaches combining *ortho*-fluorination with axial chirality to azobenzenes have been reported exhibiting helicity control upon visible light irradiation (**14**)[34a] or a long lifetime of *cis*-isomers (**15** in Table 1).[34b] Especially, incorporating two *ortho*-fluorinated azobenzenes to the central binaphthyl azobenzene scaffold (**14** in Figure 9a) resulted in various configurations of the chiral dopant by phototuning isomers upon light irradiation at 365 nm, 470 nm and 530 nm (Figure 9b). Stepwise and highly reversible control of HTP between 36 (PSS_{365nm}, configuration III-rich) and 160 (PSS_{470nm}, configuration I-rich) via 112 μm^{-1} (mol%) (PSS_{530nm}, configuration II-rich) was demonstrated based on tristable chiral switch **14** (Figure 9c). Versatile phototunability of reflection colors in visible and infrared region was also obtained (Figure 9d,e).

Meanwhile, axially chiral azobenzene dopants in highly strained cyclic forms by connecting azobenzenes and binaphthyl moieties have been reported.[35] Cyclic azobenzophane dopants containing binaphthyl units (**16** in table 1) underwent helix inversion from +8 μm^{-1} (initial) to −26 μm^{-1} (PSS_{UV}) with the maximum HTP switching of 425% upon *cis*-isomerization, and recovered its original handedness upon visible light irradiation.[35a] Nishikawa and coworkers[35b] investigated helical reorganization differences between cyclic and linear dopant configurations (Figure 10a): two azo groups substituted to axially chiral binaphthyl core are either bridged through alkyl linker (**17**, closed-type) or disconnected (**18**, open-type), respectively. In host nematic LCs, the initial HTP value increased monotonically as the alkyl bridge extended from butyl to hexyl, then it decreased upon further lengthening to octyl. The authors inferred that the highest HTP value of −137 μm^{-1} was achieved with the hexyl bridged **17** with a dihedral angle of around 45°, and its helical sense was not changed after sequential irradiation at 400 (−73 μm^{-1}) and 460 nm (−109 μm^{-1}). Whereas, open-type compound (**18**) could reversibly switch HTP and invert the handedness from +80 (initial) to −6.6 (PSS_{400}) and +25 μm^{-1} (PSS_{460}) by photoisomerization. It indicates that *cisoid* conformation of **17** at PSS_{400} and PSS_{460} can be preserved by the strictly restricted rotation around the chiral axis of the binaphthyl core, which is fixed by the bridge part, but **18** adopts configurational transition from *transoid* to

© 2019 Wiley-VCH Verlag GmbH & Co. KGaA, Weinheim

Table 1. Photoresponsive chiral dopants exhibiting chirality inversion and large HTP photoswitching ratio.

Molecular structure	Entry	Host nematic LC	β [μm^{-1}] dopant *c*: [wt%][a] or mol%[b] Initial	PSS_{UV}	PSS_{Vis}	$\lvert\Delta\beta/\beta_{ini}\rvert$ [c] [%]	Ref.
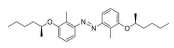	1	DON-103	−2.6[b]	−8.9[b]	−3.1[b]	242	14a
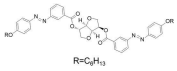	2	E44	+15.6[d]	+79.4[d]	–	409	21b
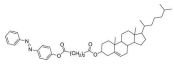	3 (n = 2)	JC-1041XX	+0.66[a]	+0.99[a]	+0.69[a]	50	26
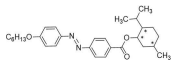	D-4	E44	+49.4[b]	+10.4[b]	–	79	27
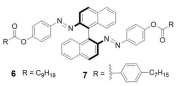	(R)-6	E7	+148[b]	+90[b]	+122[b]	39	29
	(R)-7	phase 1052	+201[b]	+106[b]	+155[b]	47	30a
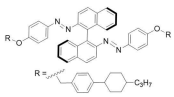	9	E7	90[a]	26[a]	58[a]	71	30c
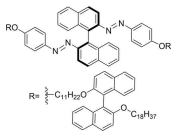	(*S*,*R*,*S*)-10	5CB	+59[b]	−65[b]	+54[b]	210	31
	(*R*,*R*,*R*)-10	5CB	+242[b]	+87[b]	+188[b]	64	31
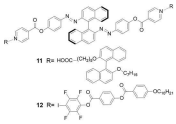	(*R*,*S*,*R*)-11	5CB	−0.39[a]	+2.80[a]	–	818	32a
	(*S*)-12	E7	136[b]	97[b]		29	32b
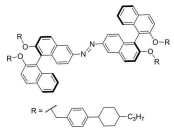	(*S*,*S*)-13	E7	52[b]	89[b] (440 nm) [e]	58[b] (550 nm) [e]	71	33
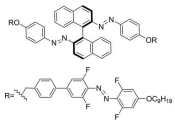	14	E7	271[b]	36[b]	160[b] (470 nm) 112[b] (530 nm) [e]	87	34a
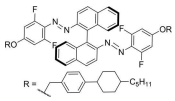	15	E7	-46.3[a]	−19.0[a]		56	34b
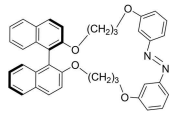	(R)-16	ZLI-1132	+8[a]	−26[a]	+6[a]	425	35a
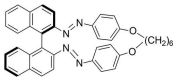	17	5CB:JC-1041XX (1:1 w/w)	−137[a]	−73[a]	−109[a]	43	35b
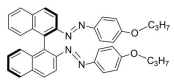	18		+80[a]	−6.6[a]	+25[a]	109	35b
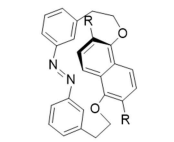	19	ZLI-1132	+40[a]	+28[a]	+36[a]	30	36a
19 R= H **20** R=Br	20	JC-1041XX	−40[a]	−16[a]	−37[a]	60	25a

© 2019 Wiley-VCH Verlag GmbH & Co. KGaA, Weinheim

These are not the final page numbers! ↗↗

Table 1. continued

Molecular structure	Entry	Host nematic LC	β [μm^{-1}] dopant *c*: [wt%][a] or mol%[b] Initial	PSS_{UV}	PSS_{Vis}	$\lvert\Delta\beta/\beta_{ini}\rvert$ [c] [%]	Ref.
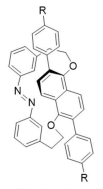 **21** R= H **22** R=C_6H_{13}	21	5CB	−72[a] −158[b]	−50[a] −110[b]	−69[a] −151[b]	31	25a
	22	5CB	−95[a] −272[b]	−47[a] −135[b]	−80[a] −229[b]	51	36d
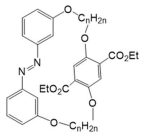 **24** n=2 **25** n=3	24	ZLI-1132	−24[a]	−11[a]	−21[a]	54	25a
	25	ZLI-1132	−21[a]	−10[a]	−19[a]	52	25a
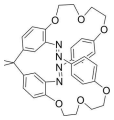	(R)-26	5CB	−6[a]	+32[a]	+26[a]	633	36e
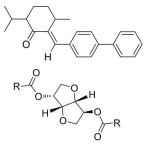	29	MBBA	−42[a]	+9[a]		121	38a
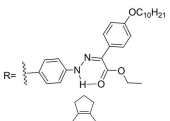	30	5CB	–	35[b] (340 nm) [e]	57[b] (410 nm) [e]	63	39b
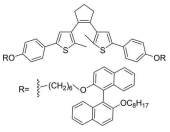	31	5CB	92[b]	77[b]	89[b]	15	41e
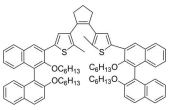	(*S*,*S*)-32	E7	+11[b]	+22[b]		100	41a
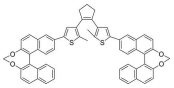	(*S*,*S*)-33	ZLI-1132	+156[b]	+173[b]		11	41a
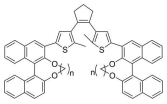	(*S*,*S*)-34 (n = 1)	5CB	+109[b]	+156[b]	+113[b]	43	41c
	(*S*,*S*)-35 (n = 2)	5CB	+228[b]	+179[b]	–	22	41d
	(*S*,*S*)-36 (n = 3)	5CB	+188[b]	+136[b]	–	28	41d
	(*S*,*S*)-37 (n = 4)	ZLI-1132	+6[b]	-25[b]	–	517	41d
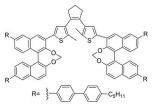	(*S*,*S*)-38	5CB	+278[b]	+223[b]	+275[b]	20	41b
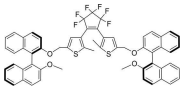	(R,R)-39	PCH	+6.6[b]	−8.3[b]	–	226	42a
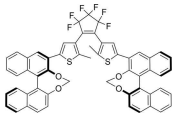	(*R*,*R*)-40	5CB	−147 [b]	−188 [b]	−150 [b]	28	42b

© 2019 Wiley-VCH Verlag GmbH & Co. KGaA, Weinheim

These are not the final page numbers! ↗↗

Table 1. continued

Molecular structure	Entry	Host nematic LC	β [μm^{-1}] dopant *c*: [wt%][a] or mol[%][b] Initial	PSS_{UV}	PSS_{Vis}	$\lvert\Delta\beta/\beta_{ini}\rvert$ [c] [%]	Ref.
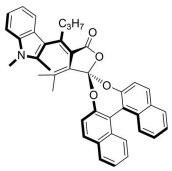	41	K15	−28[b]	−175.3[b]		526	18b
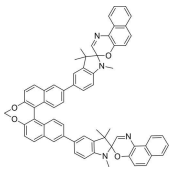	42	E7	87[b]	94[b]	–	8	17
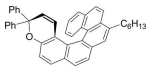	43	E7	−26.4[a]	−1.8[a]	–	93.2	20
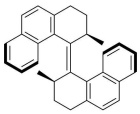	44	E7	+99[b] (*P,P*)-*trans*	+17 [b] (*P,P*)-*cis* (>280 nm) [e]	−7[b] (*M,M*)-*trans* (>280 nm) [e]	83	47b, e
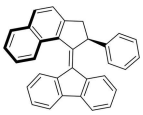	(*P*)-45	E7	+90[b]	−59[b] (*M*)-45		166	25d
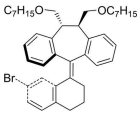	(P)-47	E7	+7.2[b]	−12.1[b] (290 nm) [e]	+6.1[b] (330 nm) [e]	268	50

[a] HTP calculated from dopant weight concentration; [b] HTP calculated from dopant molar concentration; [c] Change ratio in HTP between the initial (β_{ini}) and PSS_{UV} states; [d] HTP×10^8 m^{-1} mol^{-1} gE44; [e] irradiation wavelength.

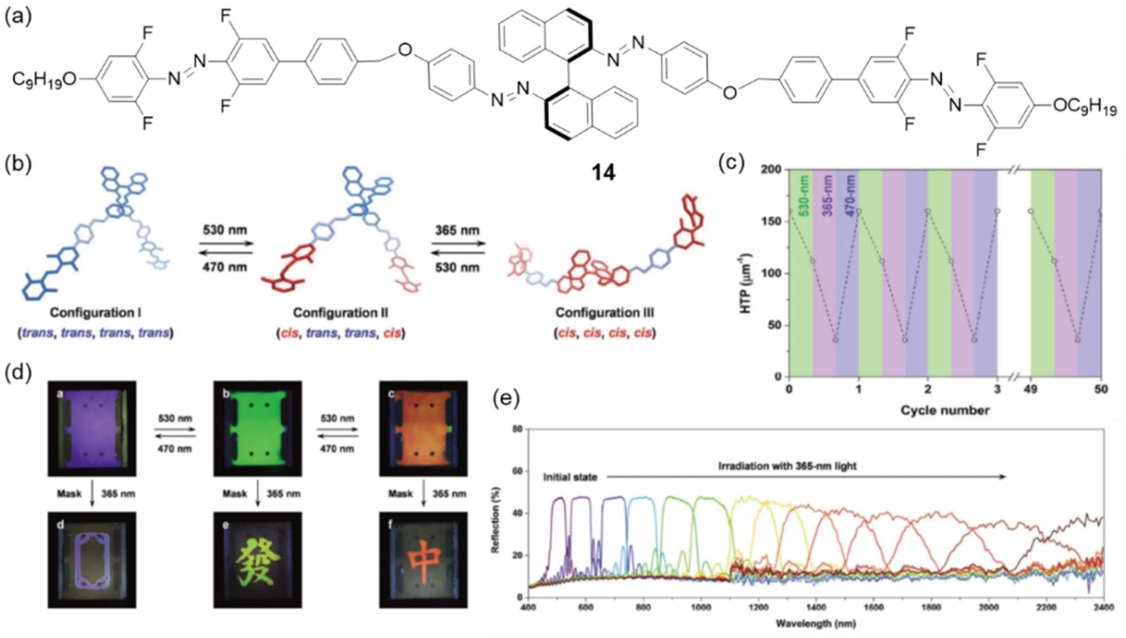

Figure 9. (a) Molecular structure of **14**. (b) Schematic illustration describing tristable configurations of **14**. *trans* and *cis* isomers are in blue and red, respectively. (c) Reversible HTP switching of **14** upon sequential irradiation at 530, 365, and 470 nm in 50 cycles. **14** in E7 in 5 μm-thick antiparallel aligned cells: (d) Real cell images showing reflection colors and photopatterns (cell containing 2.0 mol% of **14**). (e) Reflective spectral shift upon exposure to 365 nm light from the initial state (cell containing 1.0 mol% of **14**). Reproduced from Ref. [34a] with permission. Copyright 2017 Wiley-VCH.

© 2019 Wiley-VCH Verlag GmbH & Co. KGaA, Weinheim

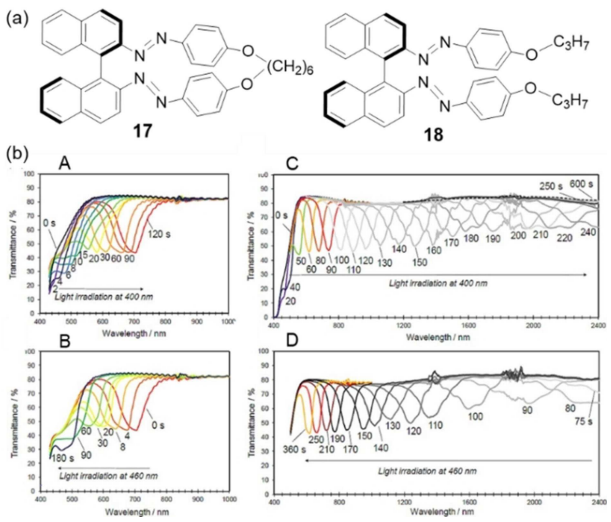

Figure 10. (a) Molecular structures of **17** (closed-type) and **18** (open-type). (b) Photocontrol of reflection spectra of 3.3 wt% **17** (A,B) and 7.0 wt% **18** (C, D) in host LCs in a planar cell at RT under light irradiation at 400 nm (top) and 460 nm (bottom). The black dotted spectrum in (C) is after irradiation at 400 nm for 600 s at the helix inversion completion. Reproduced from Ref. [35b] with permission. Copyright 2017 Wiley-VCH.

cisoid conformation after photoisomerization. In **17** (3.3 wt%) or **18** (7.0 wt%) doped CLC film, the reversible phototuning of reflection bands in visible region was confirmed for closed-type **17** (Figure 10b A,B) and helical pitch elongation to short-wave IR region followed by inversion was evidenced with open-type **18** (Figure 10b C,D) .

2.1.3. Planar Chiral Azobenzenes

In designing photoresponsive dopants, placing photoisomerizable unit and the chiral unit close to each other is preferred. Because simultaneous chiral and geometrical changes can be logically expected. Especially, the influence of photoisomerization can be largely amplified when the azobenzene moiety becomes an integrated part of the chiral core. From this point of view, one of the promising approaches to unite the photoisomerizable azobenzene and chiral unit would be the cyclization of the two units, and our group has demonstrated a series of cyclic azobenzenes forming planar chirality as chiroptical switches for the applications of reversible reflection color control, molecular brakes, and chiral memory.[25a,36] In 2008, our group reported the first planar chiral azobenzenophane dopant **19**[36a] based on asymmetric cyclophane structure bearing naphthalene and azobenzene (Figure 11). It has two enantiomers- (*R*)E-**19** and (*S*)E-**19** undergoing reversible photoisomerization to (*R*)Z-**19** and (*S*)Z-**19** without any racemization. The size of the cavity of the cyclophane in both *E* and *Z* isomers is small to prevent the free rotation of the naphthalene ring through it. Dopants show moderately high HTP values (*i.e.* $+40\ \mu m^{-1}$ in ZLI-1132 for (*R*)E-**19**), and UV irradiation resulted in HTP decrease to $+28\ \mu m^{-1}$ with a switching ratio of 30%. By

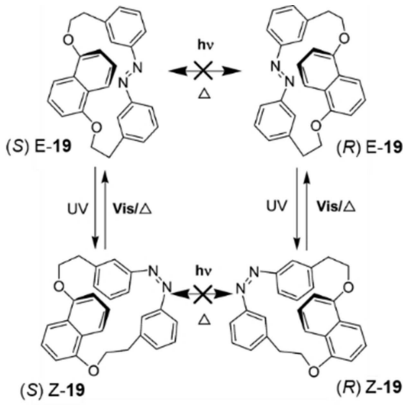

Figure 11. Photochemical and thermal processes occurring in *S* and *R* enantiomers of planar chiral **19**. Reproduced from Ref. [36a] with permission. Copyright 2008 American Chemical Society.

doping 12 wt% of (*R*)E-**19** in ZLI-1132, reversible photocontrol of the three primary colors was achieved.

A further significant improvement in the tunability of HTP was reported with a series of planar chiral azobenzenophane derivatives **19**–**25** as shown in Figure 12a.[36] In both the *E* and *Z* states of the azobenzene units, all the molecules maintain the planar chirality with separable enantiomers. Shorter spacer length and rodlike aromatic units were much beneficial to improve initial HTP values. Especially, the molecule with a bis-hexyl substituted bisphenylnaphthalene group (**22**)[36d] shows the highest ever known initial HTP of 272 μm^{-1} (mol%) among planar chiral azobenzene dopants, and the largest HTP photoswitching ratio of 60% was observed from dibrominated naphthalene substituted cyclic azobenzene (**20**).[36a] The results indicate that chiral dopants should have lower conformational freedom, higher structural rigidity, mesogenic property and structural similarity to nematic host for a larger HTP value. Significantly reduced dopant concentration of 2.4 wt% (= 0.82 mol%) was enough to demonstrate reversible photocontrol of RGB reflection colors compared with those of reported chiral photochromic dopants so far (Figure 12b).[36d] In addition, their properties as molecular machines were studied in combination with nematic LCs; HTP modulation of the chiral dopant upon photoisomerization induces dynamic rotational reorganization of the cholesteric textures at the LC surfaces. Figure 13a shows the rotational motion of a glass rod floating on the surface of a CLC formed by doping **20** (1 wt%) in 5CB upon irradiation at 366 nm (277° in an anticlockwise direction, A–D) and 436 nm (clockwise rotation, E–H).[25a] **22** with the highest mesogenic similarity to LC hosts required only 0.35 wt % of doping concentration to exhibit rotating one full cycle (360°).[36d] In all cases, a negative change in HTP from initial to Z-rich state resulted in a clockwise rotation of a glass rod, whereas that of positive change resulted in a anticlockwise rotation. Importantly, this study has revealed a relationship between HTP values and photoinduced rotation angle of the micro-objects on the cholesteric film. As shown in Figure 13b, a linear dependence was observed for the rotation angle and the ratio of the HTP difference between initial (β_{ini}) and PSS_{UV} (β_{fin})

© 2019 Wiley-VCH Verlag GmbH & Co. KGaA, Weinheim

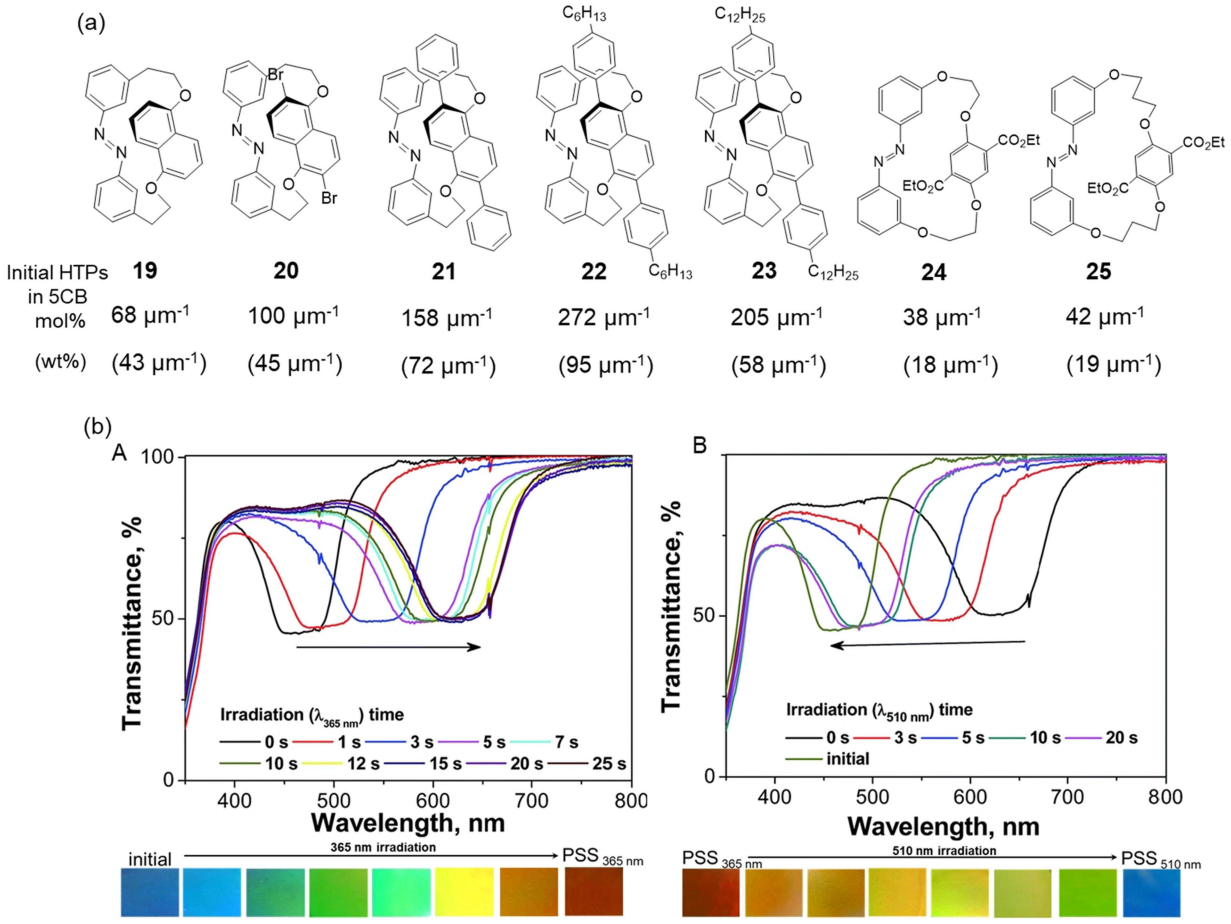

Figure 12. (a) A series of planar chiral cyclic azobenzene dopants and associated initial (*E*) state HTP values. (b) Reflection band shift and color changes of CLC film doped with 2.4 wt% (= 0.82 mol%) of **22** in 5CB upon irradiation (A) at 365 nm and (B) at 510 nm until it reaches the PSS. Reproduced from Ref. [36d] with permission. Copyright 2014 The Royal Society of Chemistry.

against the absolute value of the initial HTP ($\Delta\beta/|\beta_{ini}|$), not just the absolute value of the change in HTP between the two states ($\Delta\beta$). Additionally, it was revealed that a change in irradiation intensity hardly affects the maximum angle of the rotation, but its speed (Figure 13c).[25a]

We also reported a bicyclic azophane with planar chirality (**26**), as shown in Figure 14a. This dopant could change not only its HTP but also the handedness of a CLC reversibly by light irradiation with no molecular racemization of enantiomers occurring during the course of the photoisomerization reaction.[36e] As shown in Figure 14b, (*R*)*E*-**26** doped ZLI-1132 (1 wt%) demonstrated an achiral nematic phase (B) between the transition of the cholesteric phases with opposite handedness with continuous exposure to UV light. For this system, a photoinduced maximum HTP switching ratio of over 600% could be achieved.

2.2. Chiral Ketones

In 1995, the first chiroptical trigger for a LC which is based on a series of axially chiral bicyclic ketones was reported by Schuster et al.[19] The racemic ketone (**27**) exhibited a partial photoresolution (*ee* = 0.4%) by CPL irradiation. However, the enantiomeric enrichment unlikely resulted in the efficient transition from nematic to cholesteric phase (Figure 15a). Then, the incorporation of a mesogenic unit in the switch (**28**) could provide a system capable of reversible nematic–cholesteric phase transition upon CPL irradiation ($\lambda > 295$ nm).[37] CPL induced enantiomeric excess was 0.7% which is quite increased compared with that of **27**. HTP of photoresolved 28 was measured as 15 μm^{-1} (mol%) in nematic ZLI1167.

Several α,β-unsaturated ketones (Scheme 3f) undergoing *trans-cis* photoisomerization with C–C double bond have been utilized as light-driven chiral dopants. Especially, **29** shown in Figure 15b exhibited reversible photomodulation of pitch accompanying both HTP switching and its helix inversion.[38] Photoinduced HTP switching from $-42\ \mu m^{-1}$ (initial) to $+9\ \mu m^{-1}$ (PSS_{UV}) was observed in nematic MBBA.[38a] The oriented fingerprint textures were reversibly controlled by the interplay of opposite handedness of doped **29** and photoinactive R811 dopant in CLC film which could perform photoresponsive transmissive diffraction gratings with a period equal to the cholesteric pitch *p*. The transmitted diffraction beam through the CLC cell was photochemically steered (Figure 15c).[38b]

© 2019 Wiley-VCH Verlag GmbH & Co. KGaA, Weinheim

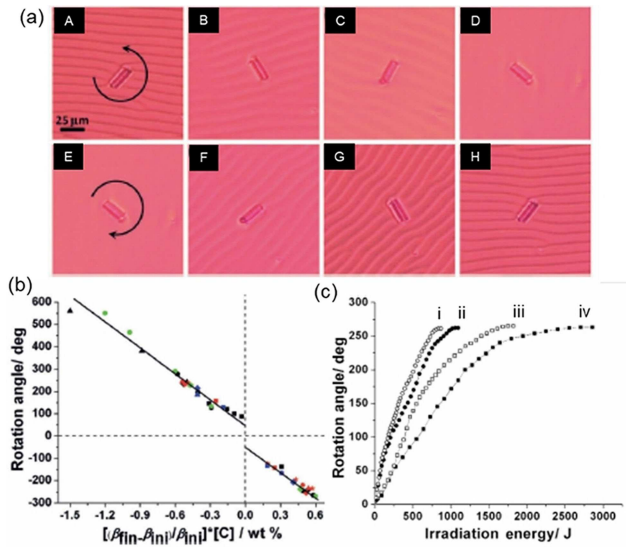

Figure 13. (a) POM images recorded at intervals of 15 s showing the rotation of a glass rod on the surface of a CLC film doped with **20** (1 wt%) in 5CB: upon irradiation at 366 nm (A–D) and at 436 nm (E–H). (b) Angle of each rotation plotted against the HTP photoswitching ratio and the chiral dopant concentration. The positive and negative values in angle indicate clockwise and anticlockwise rotation of the glass rods, respectively. The dopants are represented as **20** (dot), **21** (square), **24** (triangle) and **25** (diamond). The nematic LC hosts are featured in different colors: 5CB (black), E-7 (blue), ZLI-1132 (red) and JC-1041XX (green). (c) Irradiation-energy-dependent angle of rotation upon irradiation with light of 436 nm at different light intensities (i) 30.4, (ii) 14.4, (iii) 7.9 and (iv) 2.8 mW cm^{-2}. Reproduced from Ref. [25a] with permission. Copyright 2012 Wiley-VCH.

2.3. Chiral Hydrazones

Recently, Aprahamian et al. developed a novel family of Z–E photoisomerizable hydrazone-based compounds.[39] By replacing the pyridyl rotor part of parent hydrazone switch with a phenyl one, the authors could obtain long-living negative photochromic compounds exhibiting thermal half-lives up to 2700 years. Then, they introduced an isosorbide scaffold to this photochromophore to build a new chiral dopant (**30**) for photoresponsive bistable cholesteric LC film (Figure 16).[39b] Depending on the irradiation wavelength in the range from 340 to 410 nm, doped CLC film showed different HTP values. Maximum HTP value was observed as 57 μm^{-1} (mol%) in 5CB upon irradiation at 410 nm and it decreased to the minimum value of 35 μm^{-1} (mol%) upon 340 nm light irradiation. Although the doped CLC films could not exhibit light reflection in the visible region even at a high doping concentration of 27 wt%, it could modulate the light reflection in the near-infrared region and also kinetically lock the PSS-defined helicity of the CLC. The dopant showed unprecedented photo-induced cholesteric to chiral smectic (SmA*) phase transition in nematic host (Figure 16b), which was utilized to photochemically control the opacity of a thin LC film as shown in Figure 16c.

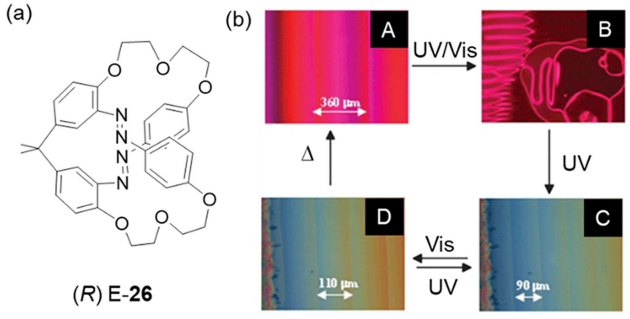

Figure 14. (a) Structure of bicyclic azophanes **26**. (b) POM images of a Cano wedge cell filled with **26** in ZLI-1132 at RT: (A) before irradiation, (B) nematic phase after the exposure to either UV or visible light irradiation, (C) PSS$_{UV}$ and (D) PSS$_{vis}$. Reproduced from Ref. [36e] with permission. Copyright 2009 The Royal Society of Chemistry.

2.4. Chiral Diarylethenes

Photoisomerizable diarylethenes undergo a reversible π electron cyclization (open-form to closed-form) upon light irradiation and show considerable changes in structure and electronic configuration (Scheme 3b). They are of particular interest as photo-responsive chiral dopants for CLCs because of their outstanding fatigue resistance and thermal stability of the isomers. The Feringa group and the Irie group demonstrated chiral diarylethene dopants by substituting chiral imine, cholesterol or chiral binaphthyls.[40] Due to their quite low intrinsic HTP values, phase transition between cholesteric and achiral nematic phases was usually obtainable.[40a] Since 2011, significant progress has been made with chiral dopants based on diarylethenes in terms of high HTP and its photoinduced large switching including a handedness inversion. Binaphthyl moieties have been considered as one of the powerful helicity inducers in achiral nematic hosts as depicted in the previous section. Thus, fine structural tuning of axially chiral binaphthyl unit and its coupling to photoisomerizable diarylethene core can lead to a large HTP as well as stable photoswitching properties.

Among widely studied modification of the binaphthyl units, there are noteworthy strategies such as placing axially chiral binaphthyl moiety closer to photoisomerizable diarylethene,[41a] extending mesogenic part,[41b] and bridging binaphthyl units[41c,d]- overall attempted by the Li group- which brought significant improvement in the compatibility with nematic host or the highly strained chiral conformation. Their representative chiral dopants (**31**–**38**) are shown in Figure 17. The considerably high HTPs were observed with the compounds bearing bridged binaphthyl units (**33**–**38**).[41b–d] These bridged moieties can induce cholesteric phase much efficiently rather than those of unbridged ones (**31**,**32**)[41a,e] because of their rigid structure and relatively narrow dihedral angle (around 60°). In terms of the handedness of the doped CLC, *S* configuration binaphthyl derivatives normally induces a left-handed helix with $\theta > 90°$, while right-handedness is observed with $\theta < 90°$. Interestingly, **33**[41a] and **34**[41c] bearing the shortest bridge length showed a significant increase of HTPs upon UV irradiation. The authors attributed this phenomenon to the changes in dihedral angle and the overall molecular conformation caused by photo-isomerization. A slight variation in the dihedral angle is also possible ($\Delta\theta$ of around 5°) even though the binaphthyl units are fixed with a methylene tether with low flexibility.[41c]

© 2019 Wiley-VCH Verlag GmbH & Co. KGaA, Weinheim

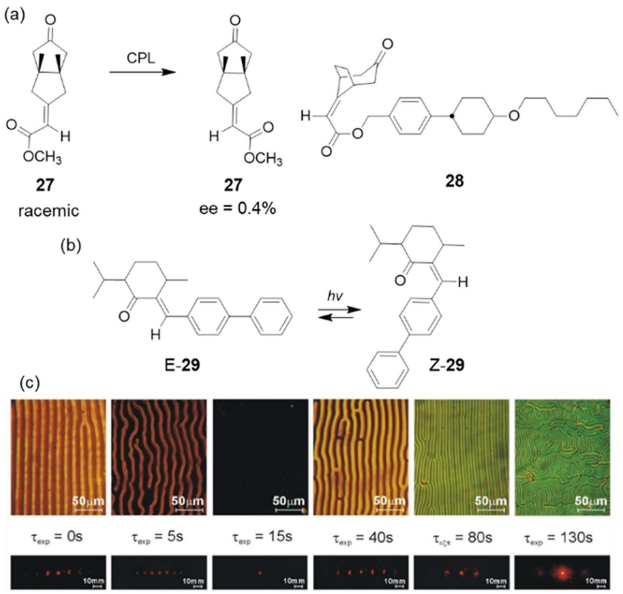

Figure 15. (a) Bicyclic ketones (**27** and **28**) which can undergo partial photoresolution by CPL irradiation. (b) Photoisomerization of helix invertible α,β-unsaturated ketone (**29**). (c) Images of aligned fingerprint textures (gratings) generated after different exposure times and diffraction patterns corresponding to formed gratings. Reproduced from Ref. [38b] with permission. Copyright 2012 Optical Society of America.

Meanwhile, the highest initial HTP value of 278 μm^{-1} (mol%) was achieved with compound **38** in 5CB[41b] consisting of highly strained bridged binaphthyl units and rigid mesogenic moieties. In general, 5 ~ 7 wt% of dopant concentrations were required to obtain RGB reflection colors and their photoswitching in doped CLCs (Figure 18).

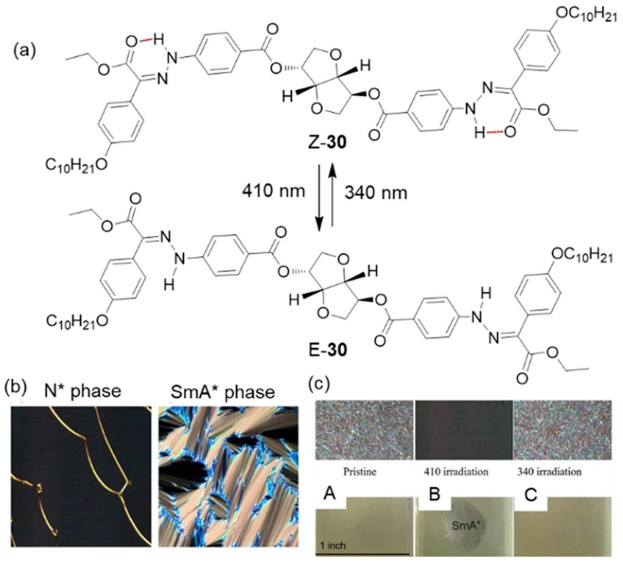

Figure 16. (a) Photoisomerization of **30**. (b) POM images of **30** in 5CB in a homogeneously aligned cell: cholesteric phase and SmA* phase induced by irradiation at 340 nm and 410 nm light, respectively. (c) Optical window where (A) the pristine cholesteric phase scatters light, (B) upon 410 nm light, the homeotropically aligned SmA* phase is optically transparent, and (C) the re-formed cholesteric phase upon 340 nm light scatters light again. Reproduced from Ref. [39b] with permission. Copyright 2018 American Chemical Society.

Some chiral diarylethene derivatives showed photochemical chiral phase induction or helix inversion of doped CLCs. Akagi et al. reported the first dynamic photocontrol of helical inversion in CLCs based on a dithienylperfluorocyclopentenes derivative containing two axially chiral binaphthyl moieties (**39**).[42a] Upon UV and visible light irradiation, photoisomerization induces a reversible dihedral angle change of the binaphthyl rings. In case the binaphthyl moiety bears the shortest alkyl chain length (**39**), the doped CLC exhibited reversible handedness switching between the open and closed forms of the dithienylethene unit (Figure 19b). Li et al.[42b] presented that axially chiral dithienylperfluorocyclopentene (**40**) shows a nematic-like phase at a very low doping concentration, such as 0.1 mol% in 5CB, which accompanies reversible isothermal phase transition between nematic and cholesteric phases upon light irradiation (Figure 19c).

Li and coworkers also demonstrated helix invertible CLCs based on bridged binaphthyl-substituted dithienylcyclopentenes with a bridge length of $n=4$ (**37**).[41d] Those of shorter bridge lengths ($n=1\sim3$, **34–36**)[41c,d] exhibited higher initial HTP values but smaller switching ratio maintaining its handedness upon photoinduced ring-closure process (Table 1). Therefore, increasing bridge length may improve the molecular flexibility and phototunabilities. In their report, **37** introduced in 5CB, E7, or ZLI-1132 showed right- to left-handedness inversion upon UV light irradiation. The highest initial HTP of 54 μm^{-1} (mol%) was obtained in 5CB, and maximum HTP switching ratio of 517% was observed in ZLI-1132. These photoinduced large HTP switching and handedness inversion are plausibly attributable to the large increase in the θ value of (*S,S*)-**37** during the open to ring-closure process. The authors applied this handedness invertible dithienylcyclopentene dopant (**37**) for several optical applications. In addition to the reflection color control and NIR light-induced handedness inversion, **37** coupled with upconversion nanoparticles in CLC was utilized as a handedness switchable NIR transducer.[41f]

Moreover, **37**-doped CLC was employed for the 3D control of the helical axis based on its unique helical sense inversion associated with a dynamic reorganization of the entire superstructure as represented in Figure 20.[43] UV light irradiation at 310 nm to the CLC filled planar cell induced the helix rearrangement from its original standing helix (SHs) through the unwound homogeneous state and the SH with opposite handedness to the lying helix (LH; Figure 20a). Transmitted light diffraction through a bilayer CLC sample allowed them to confirm the resultant helix transition as shown in Figure 20b. The direct visualization of the dimensionality transformation could be achieved between 2D, 1D, and the diffraction-off states.[43a] Besides, the authors recently showcased the dynamically deformable and reconfigurable zigzag pattern based on (*S,S*)-**37** (3.7 wt% in E7) under the simultaneous application of an electric field and light (Figure 21).[43b] Straight and zigzag patterns could be emerged and dissipated repeatedly on demand, and could easily be modified by switching irradiation with UV and visible light. The facile and cohesive tunability of

© 2019 Wiley-VCH Verlag GmbH & Co. KGaA, Weinheim

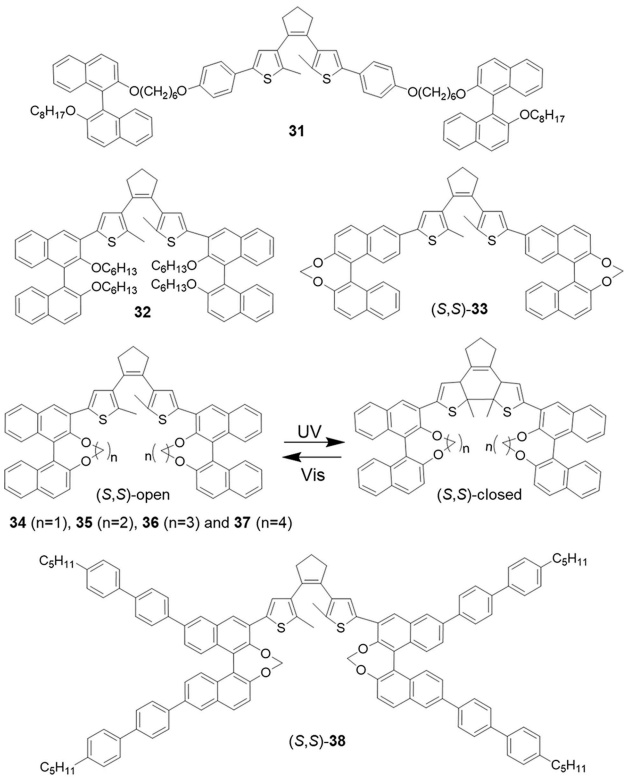

Figure 17. A series of chiral diarylethenes (31–38) bearing axially chiral binaphthyl moieties.

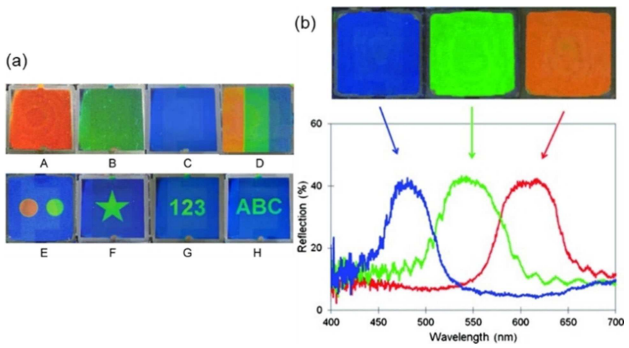

Figure 18. RGB reflection colors and photopatterns observed from CLC filled cell: (a) (*S,S*)-**34** in E7 (7.7 wt%). Reproduced from ref.[41c] with permission. Copyright 2012 American Chemical Society; (b) 1.3 mol% (*S,S*)- **38** in 5CB and corresponding reflection spectra upon UV irradiation at 310 nm for 0 s (red), 20 s (green), and 60 s (blue). Reproduced from Ref. [41b] with permission. Copyright 2014 Wiley-VCH.

the helical axis of CLC can be beneficial aspect for advanced 3D photonic devices.

2.5. Chiral Fulgides

It is known that fulgides undergo a bond rearrangement leading to the transition from the open form (E-form) to the closed form (C-form) by UV light irradiation, and the reverse process takes place by visible light irradiation as shown in

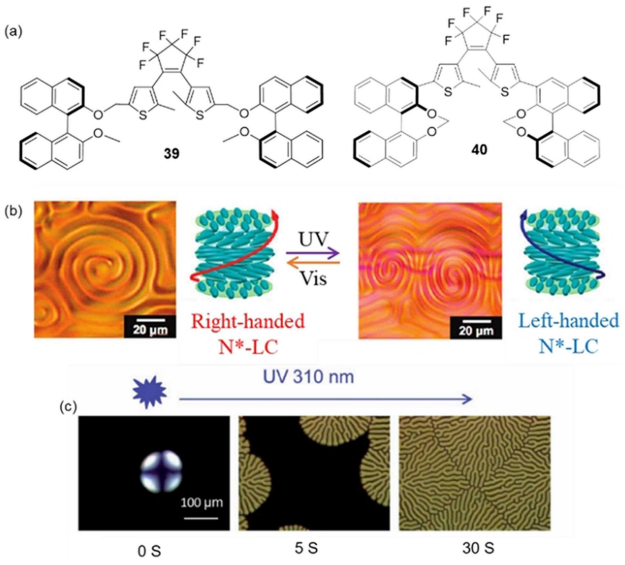

Figure 19. (a) Dithienylperfuorocyclopentenes (*R,R*)-**39** and (*R,R*)-**40** with axially chiral bisbinaphthyl substitution. (b) POM observed cholesteric texture transition of CLCs containing (*R,R*)-**39** (1.0 mol%) between the open form (left) and PSS (right) upon UV ($\lambda = 254$ nm) and visible ($\lambda > 400$ nm) light irradiation. Reproduced from ref.[42a] with permission. Copyright 2012 American Chemical Society. (c) Cross-polarized optical textures of (*R,R*)-**40** in 5CB (0.1 mol%) upon UV irradiation from 0 s (conoscopic observation) to 30 s. Reproduced from Ref. [42b] with permission. Copyright 2013 The Royal Society of Chemistry.

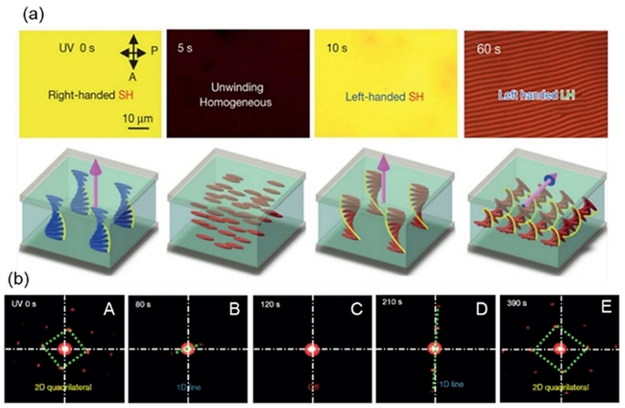

Figure 20. (a) UV irradiation to a planar cell filled with a chiral switch (**37**)-doped CLC transforms its original standing helix (SH), through the non-helical homogeneous state and the SH arrangement with opposite handedness, to the lying helix (LH). (b) Diffraction dimensionality transformation of a bilayer CLC sample. Diffraction patterns were transformed upon continuous UV light exposure from two-dimensional (2D; A), through one-dimensional (1D; B) and the diffraction off state (C), to 1D again (D), and finally to 2D (E). Reproduced from Ref. [43a] with permission. Copyright 2016 Nature Publishing Group.

Scheme 3e. As responsive chiral dopants, chiral indolylfulgides have been employed which could provide long cholesteric pitch upon photoisomerization.[18,44] Yokoyama et al reported that the incorporation of a chiral binaphthol unit in the fulgide (**41**) resulted in a bistable system because of thermally stable closed-form. Besides, dramatic contrast in HTP was achieved between the open and closed forms of **41**, switching from −28 to −175.3 μm^{-1} (mol%) in K15 upon UV light irradiation,

© 2019 Wiley-VCH Verlag GmbH & Co. KGaA, Weinheim

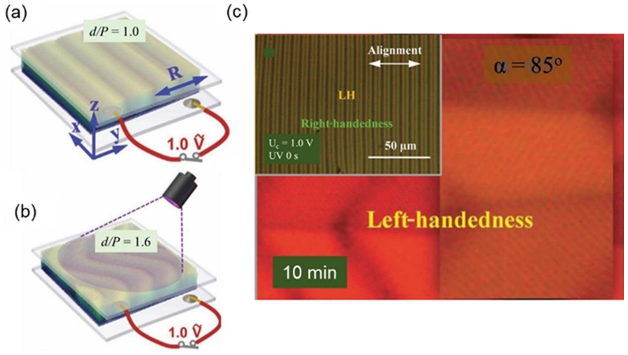

Figure 21. Generation of a straight (a, inset of c) and zigzag-shaped patterns (b, c) based on the CLC containing **37** through the combination of light irradiation and electric field application at a constant voltage $U_c = 1.0$ V (1 kHz). Reproduced from Ref. [43b] with permission. Copyright 2017 Wiley-VCH.

respectively (Figure 22a).[18b] In addition, based on its unique bistability, the temporal stability of the reflection band at arbitrary spectral positions was demonstrated representing its long-lasting, optically reconfigurable color changes.[44b]

2.6. Chiral Spirooxazines

Ring-closed forms (colorless) of spiropyran and spirooxazine can be transformed into the zwitterionic merocyanine open-form (colored) upon UV light irradiation, and its reverse process proceeds thermally in the dark or photochemically by visible light irradiation (Scheme 3d). As a chiral dopant for photo-responsive CLC, a series of axially chiral spirooxazines has been reported by the Li group.[17] In their molecular design, bis-spirooxazine was substituted to an axially chiral binaphthyl

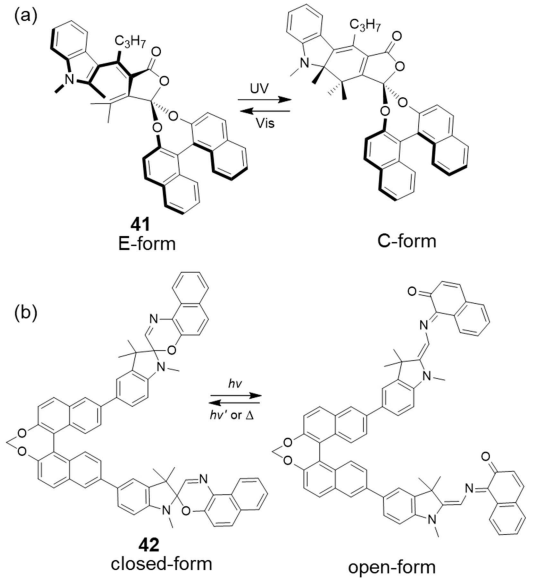

Figure 22. Photoisomerization of (a) chiral indolylfulgide dopant (**41**) and (b) chiral spirooxazine dopant (**42**).

moiety which is one of the strong helical inducers. Chiral spirooxazines showed fast thermal relaxation to the initial state. Especially, a chiral dopant bearing bridged binaphthyl moiety (**42**) shown in Figure 22b exhibited the highest initial HTP value of 87 μm^{-1} (mol%) in E7 and it became larger to 94 μm^{-1} (mol %) upon irradiation with UV light (365 nm). Whereas for other chiral spirooxazines, HTP decreased under the same condition. It is probably originated from the smaller dihedral angle between the two naphthalenes of the bridged compound which leads to a more rodlike structure in the merocyanine form.[17]

2.7. Helicene-Like Naphthopyrans

Helicene-like molecules have intrinsically robust helical conformation which can effectively transfer their chiral information to the nematic host.[45] Whereas, photoisomerizable helicene compounds as photoresponsive dopants are rather unexplored compared with photochemically reversible P-type molecules, such as azobenzenes and diarylethenes. Recently, novel photochromism of helicene-like naphthopyrans has been reported to overcome fast thermal relaxation.[46] As shown in Figure 23, the

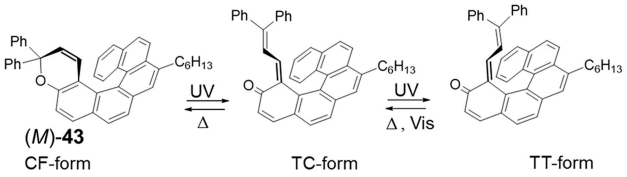

Figure 23. Reversible photoisomerization of (*M*)-**43**: closed form (CF), transoid-cis (TC) and transoid-trans (TT).

closed ring form (CF) of **43** changes to open form upon UV irradiation.[20] The *transoid-trans* (TT) isomer is the major photoproduct at the photostationary state upon continuous irradiation, and is more thermodynamically stable than the metastable *transoid-cis* (TC) form. Open forms can reconvert to the CF both thermally and upon visible light irradiation.

Upon UV light irradiation to **43** doped in E7, dramatic helical pitch elongation occurred as shown in Figure 24 A,B. The initial HTP value of $-26.4\ \mu m^{-1}$ was decreased to $-1.8\ \mu m^{-1}$ which led to the unprecedented large photoswitching of HTP over 93%.[20] It is ascribed to a large conformational transition from a [6]-helicene to a [5]-helicene like molecule with a bulky dienic unit at the 1-position. Consequently, TT form reduces its chirality transfer to the host medium accompanying huge decrease of HTP due to the largely perturbed and elongated helical conformation. In addition, its dynamically self-organizable CLC (0.2 wt% of **43** in E7) produced mechanical work of a micro-object with light energy.[20] As shown in Figure 24C, fingerprint textures were rotationally reorganized and finally almost faded by reaching TT-rich state (h) of **43** accompanying the counter-clockwise rotation of a glass rod. Afterward, dissipated fingerprint texture gradually emerged again and the glass rod rotated in a clock-

© 2019 Wiley-VCH Verlag GmbH & Co. KGaA, Weinheim

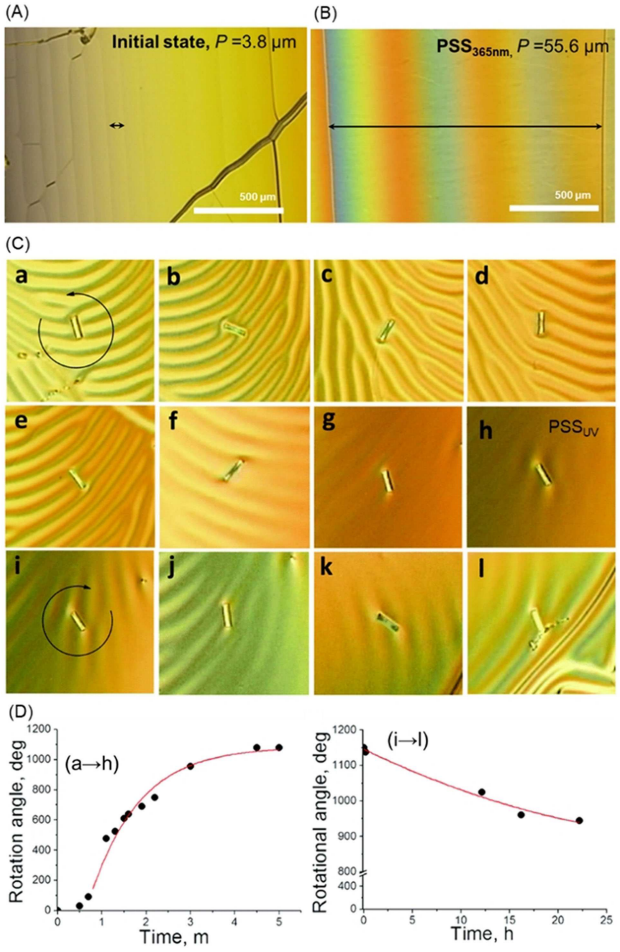

Figure 24. Cano wedge cell images with Cano lines obtained from 1 wt% **43** in E7: (A) initial and (B) PSS_{365nm}. (C) POM images of the rotational motion of a glass rod on the surface of the CLC film (0.2 wt% of **43** (*M*) in E7): from (a) to (h) upon continuous UV light irradiation for 5 min, counter-clockwise rotation; from (i) to (l) upon thermal back process at room temperature, clockwise rotation. (D) Rotation angle change during the process of (a–h) and (i–l). Reproduced from Ref. [20] with permission. Copyright 2017 The Royal Society of Chemistry.

wise direction upon thermal back process (i to l). Figure 24D depicts the rotational angle change observed during the whole (a-l) process. The rotation became fast when it passed the threshold at around 40s, presumably exceeding the boundary energy to have TT form. Upon continuous irradiation, the rotation speed reduced and eventually stopped by reaching the photostationary state of the dopant, and almost 3 full cycles (1150°) were achieved (a to h). Compared with the reports based on overcrowded alkene (900° at 1 wt%),[25d] central chiral azobenzene (1200° at 6 wt%)[25b] or planar chiral azobenzene (360° at 0.35 wt%)[36d] dopants, the largest photo-induced rotational angle per unit concentration was achieved with **43**, which is beneficial to provide an efficient molecular machinery system. Furthermore, unlikely to other photoresponsive CLC system, the high thermal stability of the TT form encountered a very slow backward rotation (i to l, 18% rotation angle recovery in 22 hours) which has function of bistable memory of rotation angles.

2.8. Overcrowded Alkenes

Sterically overcrowded alkene with intrinsic helical conformation processes a stereogenic center at the rotor part and a fluorene group at the stator part.[14c,47] The photoisomerization around the C=C double bond of this chiral switch is known to invert its molecular helicity (Scheme 3c). Since the first demonstration on overcrowded alkene-based switches witnessing handedness inversion of doped cholesteric phases by Feringa et al.,[47a] a series of overcrowded alkene derivatives has been developed and its mechanism could be elaborated which includes four stages of photochemical and thermal isomerization.[47b] Figure 25 shows the unidirectional rotation

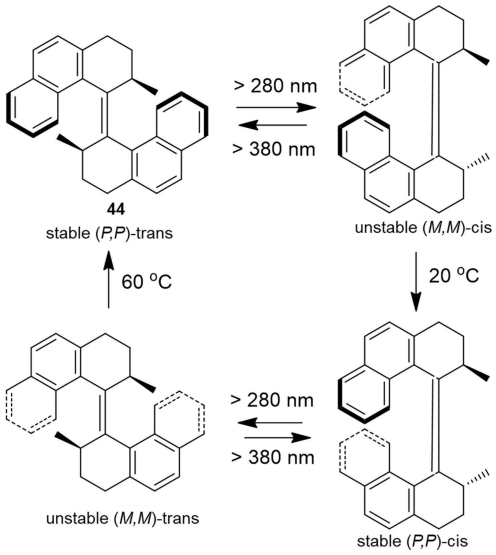

Figure 25. Unidirectional rotation process of molecular motor **44**.

process of overcrowded alkene which is known as the first-generation molecular motor (**44**). The HTP (mol%) of the stable (*P*,*P*)-trans form of **44** was $+99\ \mu m^{-1}$ in E7 and its (*P*,*P*)-cis form showed $+17\ \mu m^{-1}$. Whereas, generation of a cholesteric helix with an opposite sign of similar HTP value was impossible, as only the (*M*,*M*)-trans form shows rather smaller HTP of $-7\ \mu m^{-1}$ (mol%). **44** doped CLC film could induce irreversible (redshift) reflection color transition based on the photochemical and thermal HTP modulation.[47b,e]

Figure 26a features a reversible isomerization process of representative overcrowded alkene derivatives (**45**,**46**), which have broadened the application of their unique photonic and mechanical functions.[25c–e,48] **45** showed quite large HTPs (mol %) for both stable ($+90\ \mu m^{-1}$ in E7) and unstable ($-59\ \mu m^{-1}$ in E7) forms by introducing fluorene moiety which possibly contributed to better structural compatibility with the LC host biphenyl core. Irradiation with UV light results in its switching from *P*-helicity to *M*-helicity.[48] Yet, the isomer with *M*-helicity is not thermally stable, hence the non-photochemical transition occurs from *M*- to *P*-helicity. CLC film doped with 1 wt% **45** in E7 formed self-organized surface relief gratings- fingerprint textures (20 nm in height, Figure 26b). The corresponding light-

© 2019 Wiley-VCH Verlag GmbH & Co. KGaA, Weinheim

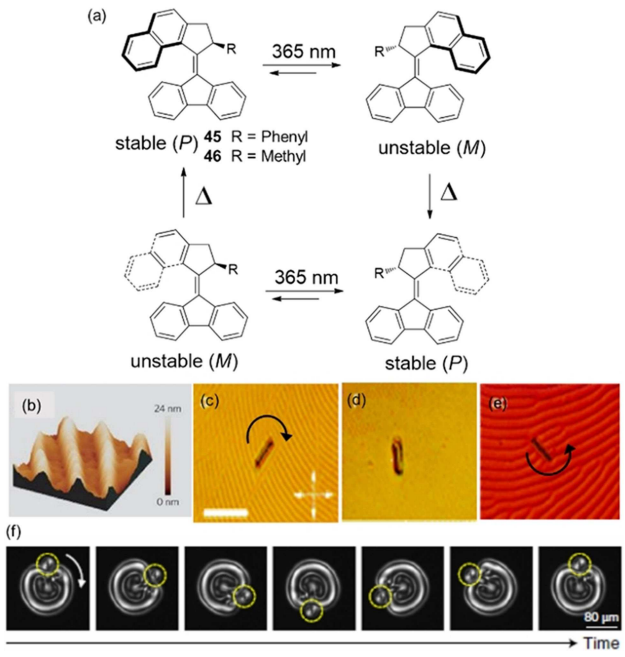

Figure 26. (a) A unidirectional rotary cycle of the fluorene-based motor. (b) The surface structure of the LC film (atomic force microscopy image; 15 μm^2). Optical micrographs of a glass rod rotating on an LC film doped with **45**, upon irradiation with UV light ($\lambda = 365$ nm): (c) The rod and the cholesteric texture rotate in a clockwise fashion; (d) Cholesteric texture does not appear during helix inversion of the motor; (e) The rod and the cholesteric texture rotate in a counter-clockwise fashion after the helix inversion. (f) Off-axis rotational transport of a particle-like LC structure: an orbiting trajectory under the effect of the photoinduced revolving pattern of fluorene-based motor doped CLC. The rotation period is around 23 min. (b) Reproduced from Ref. [25c] with permission. Copyright 2006 Nature Publishing Group; (c-e) Reproduced from Ref. [25d] with permission. Copyright 2006 American Chemical Society; (f) Reproduced from Ref. [49a] with permission. Copyright 2018 Nature Publishing Group.

directing helix unwinding and handedness inversion were observed upon irradiation with UV light, and the reverse process spontaneously proceeds at room temperature. When reaching the helix inversion point, an achiral (compensated) nematic phase was generated without a cholesteric fingerprint texture (Figure 26d) followed by the rewinding of the cholesteric helix with an opposite handedness upon continuous irradiation (Figure 26e). Especially, opposite rotational direction of a micro-sized glass rod on the CLC film was observed via static movement state according to the handedness change of CLC. It reflects that molecular level chirality change could be translated to the macroscopic level (Figure 26c–e). In a further study, White et al.[48a] and Aßhoff et al.[48b] clarified the reversible and broad tunability of overcrowded alkenes-based CLCs in terms of its helical pitch length and photoinvertible handedness.

Recently, **45** or **46** based helix invertible CLCs were utilized to achieve unique continuous and unidirectional rotational of LC structure in a confined system.[49] At the supramolecular level, the cholesteric texture rotation was sustained by the diffusion of the motors away from the localized illumination spot (Figure 26f). It indicates that the interplay of the cholesteric structure and the diffusion of the photoresponsive chiral dopant is a key to achieve a continuous, regular and unidirectional rotation under non-equilibrium and spontaneous symmetry breaking conditions.[49a]

Chen et al. reported 10,11-disubstituted dibenzeosuberane (DBS)-based helicenes (**47**) exhibiting molecular helicity inversion upon photoisomerization (Figure 27).[50] The induced cholesteric

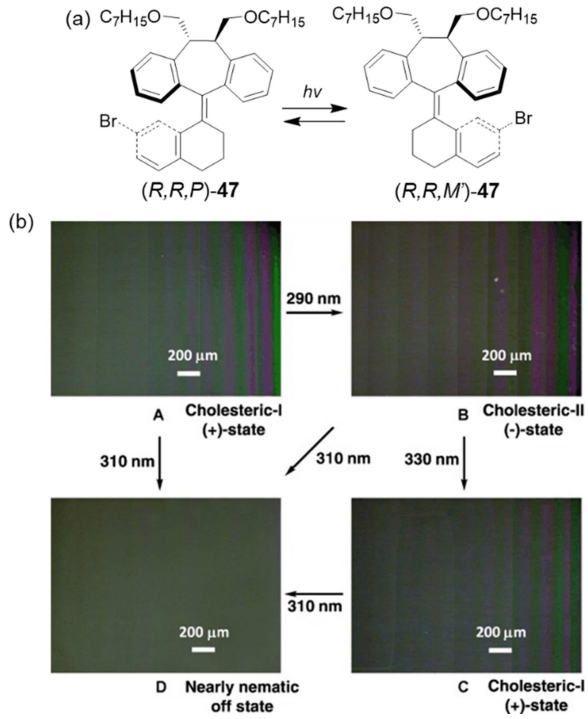

Figure 27. (a) Photoisomerization of the system 10,11-disubstituted dibenzeosuberane-based helicenes **47**. (b) A wedge cell, shown by POM images, filled with (*P*)-**47** (1 wt%) doped E7 upon UV irradiation: (A) initial state; (B) after irradiation at 290 nm for 3 h; (C) after subsequent irradiation at 330 nm for 2 h; (D) after irradiation at 310 nm for 3 h. Reproduced from Ref. [50] with permission. Copyright 2010 Wiley-VCH.

phase in nematic E7 was also found to undergo light-driven handedness inversion by sequential UV light irradiation at different wavelengths such as 290, 310, and 330 nm. In this system, the conformation control of the top DBS template is a key to the selective photoswitching in cholesteric mesophase. Hence, the alternating irradiation at those three wavelengths led to a diverse photomodulation of the pitch length, handedness reversal and chirality-off mode (Figure 27b).

Meanwhile, overcrowded alkene derivative which can undergo partial photoresolution within a nematic LC (Scheme 2iii,iv) has been reported by Feringa and coworkers.[51] The photoisomerization process resulted in the formation of a cholesteric phase upon CPL irradiation. From the racemic compound, one of the enantiomeric forms- *P* or *M* could be enriched by *r*-CPL or *l*-CPL irradiation, respectively. They could also interconvert by CPL irradiation of opposite handedness at 313 nm (Figure 28). Due to the low photochemical enantiomeric excess of 0.07% and low HTP of (*M*)-**48** (0.1 μm^{-1} in M15), a high dopant concentration of around 20 wt% was required to observe a cholesteric texture. However, their finding on photoinduced chirality and its versatile

© 2019 Wiley-VCH Verlag GmbH & Co. KGaA, Weinheim

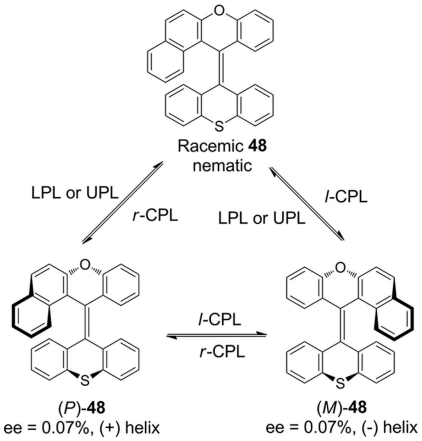

Figure 28. Enantiomeric excess induced by CPL irradiation of overcrowded alkene-based molecule **48** in a nematic LC resulting in three-stage switching.

manipulation provided deeper insights regarding how molecular chirality can be amplified influencing macroscopic reorganization of LC medium.

3. Summary and Outlook

This Review highlights the recent progress on photoresponsive low molecular weight cholesteric LCs aiming to achieve advanced optical and mechanical functions. Reports on photochemical pathways to transfer chiral information to the host medium have been considered. In particular, chiral photochromic dopants are focused upon, a system which can effectively organize achiral nematic LCs into optically active self-assembled helical superstructures at very low doping levels and which enable a dynamic control of the photophysical properties of the entire host medium based on the photoisomerization reaction. Light-driven dynamic modification of supramolecular chirality includes helical pitch length control, handedness inversion and even chirality induction from achiral (racemic) LCs. An intrinsic helical twisting power and its switching upon photoisomerization of a chiral dopant within a CLC significantly influences the degree to which the helical pitch length, director orientation and handedness can be manipulated. A particular important aspect of the presented research works is that as well as achieving a photoinduced chiral transition, it is also possible to amplify and express the chiral information at various scales. These materials may offer major advantages for photo-mediated chiral materials as well as in advanced photonics applications, such as, for example, reflective displays, optical shutters, reflectors, diffractors, optical storage and for attaining macroscopic work.

Nevertheless, a precise prediction of which system would offer certain targeted chiroptical or mechanical properties still remains a challenge. Some trends and information have been obtained when considering the relationship between molecular structure and helical twisting power or handedness, but it is highly difficult to realize chirality amplification of a macroscopic event accompanying continuous supramolecular reorganization ("motor-like" function). Integrating efforts to unveil the underlying principle which bridges the gap between nanoscale molecular events and macroscale phenomena and the development of novel photochromic switches would provide general rules and guidelines to obtain the desired target functions from chiral supramolecular systems.

Acknowledgements

This work was partly supported by JSPS KAKENHI Grant Number JP16 K17886, Toyo Gosei Memorial Foundation and Mazda Foundation.

Conflict of Interest

The authors declare no conflict of interest.

Keywords: chiral dopants · chirality · cholesteric liquid crystals · helical twisting power · photoresponsive systems · photoswitches

[1] a) M. Liu, L. Zhang, T. Wang, *Chem. Rev.* **2015**,115, 7304–7397; b) M. A. Mateos-Timoneda, M. Crego-Calama, D. N. Reinhoudt, *Chem. Soc. Rev.* **2004**, *33*, 363–372; c) E. Yashima, N. Ousaka, D. Taura, K. Shimomura, T. Ikai, K. Maeda, *Chem. Rev.* **2016**, *116*, 13752–13990.
[2] a) X. Yan, F. Wang, B. Zheng, F. Huang, *Chem. Soc. Rev.* **2012**, *41*, 6042–6065; b) G. Qing, T. Sun, *NPG Asia Mater.* **2012**, *4*, e4, 1–13.
[3] R. M. Tejedor, L. Oriol, J. L. Serrano, T. Sierra, *J. Mater. Chem.* **2008**, *18*, 2899–2908.
[4] a) Y. Kim, N. N. Mafy, N. Tamaoki, *Photoactive Functional Soft Materials*: Photochemical Chirality Induction and Inversion in Soft Materials **2019** Wiley-VCH (Eds. Q. L.); b) H. K. Bisoyi, Q. Li, *Angew. Chem. Int. Ed.* 2016, 55, 2994–3010; *Angew. Chem.* **2016**, *128*, 3046–3063; c) H. K. Bisoyi, T. J. Bunning, Q. Li, *Adv. Mater.* **2018**, *30*, 1706512; d) H. K. Bisoyi, Q. Li, *Chem. Rev.* **2016**, *116*, 15089–15166; e) L. Wang, A. M. Urbas, Q. Li, *Adv. Mater.* **2018**, 1801335.
[5] a) T. Kosa, L. Sukhomlinova, L. Su, B. Taheri, T. J. White, T. J. Bunning, *Nature* **2012**, *485*, 347; b) N. Tamaoki, G. Kruk, H. Matsuda, *J. Mater. Chem.* **1999**, *9*, 2381; c) Y. Kim, M. Wada, N. Tamaoki, *J. Mater. Chem. C*, **2014**, *2*,1921-1926.
[6] a) R. A. M. Hikmet, H. Kemperman, *Nature* **1998**, *392*, 476–479; b) T. J. White, R. L. Bricker, L. V. Natarajan, V. P. Tondiglia, L. Green, Q. Li, T. J. Bunning, *Opt. Express* **2010**, *18*, 173–178.
[7] a) J. Schmidtke, S. Kniesel, H. Finkelmann, *Macromolecules* **2005**, *38*, 1357–1363; b) L. De Sio, G. Palermo, V. Caligiuri, A. E. Vasdekis, A. Pane, J.-W. Choi, L. Maffli, M. Niklaus, H. R. Shea, C. Umeton, *J. Mater. Chem. C* **2013**, *1*, 7798–7802.
[8] a) R. A. van Delden, M. B. van Gelder, N. P. M. Huck, B. L. Feringa, *Adv. Funct. Mater.* **2003**, *13*, 319–324; b) S. Kurihara, S. Nomiyama, T. Nonaka, *Chem. Mater.* **2001**, *13*, 1992–1997.
[9] a) Y. Zhao, T. Ikeda in *Smart Light-Responsive Materials: Azobenzene-Containing Polymers and Liquid Crystals* (Eds.) John Wiley & Sons, New Jersey, **2007**; b) N. Tamaoki, *Adv. Mater.* **2001**, *13*, 1135–1147; c) T. J. White, M. E. McConney, T. J. Bunning, *J. Mater. Chem.* **2010**, *20*, 9832–9847; d) M. Moriyama, S. Song, H. Matsuda, N. Tamaoki, *J. Mater. Chem.* **2001**, *11*, 1003; e) S. Abraham, V. A. Mallia, K. V. Ratheesh, N. Tamaoki, S. Das, *J. Am. Chem. Soc.* **2006**, *128*, 7692–7698.
[10] E. Sackmann, *J. Am. Chem. Soc.* **1971**, *93*, 7088–7090.
[11] a) Kitzerow, H. Bahr, C. (eds.) (2001). *Chirality in Liquid Crystals*. New York: Springer; b) T. Nakagawa, T. Ubukata, Y. Yokoyama, *J. Photochem. Photobiol. C* **2018**, *34*, 152–191.
[12] Y. Li, M. Wang, A. Urbas, Q. Li, *J. Mater. Chem. C*, **2013**, *1*, 3917–3923.
[13] N. Katsonis, E. Lacaze, A. Ferrarini, *J. Mater. Chem.* **2012**, *22*, 7088–7097.

© 2019 Wiley-VCH Verlag GmbH & Co. KGaA, Weinheim

[14] a) C. Ruslim, K. Ichimura, *J. Phys. Chem. B*, **2000**, *104*, 6529–6535; b) C. Ruslim, K. Ichimura, *Adv. Mater.* **2001**, *13*, 37–40; c) R. Eelkema, B. L. Feringa, *Org. Biomol. Chem.* **2006**, *4*, 3729–3745.
[15] M. Irie, T. Fukaminato, K. Matsuda, S. Kobatake, *Chem. Rev.* **2014**, *114*, 12174–12277.
[16] B. L. Feringa, *J. Org. Chem.* **2007**, *72*, 6635–6652.
[17] L. Jin, Li, Y. J. Ma, Q. Li, *Org. Lett.* **2010**, *12*, 3552–3555.
[18] a) Y. Yokoyama, T. Sagisaka, *Chem. Lett.* **1997**, *26*, 687–688; b) T. Sagisaka, Y. Yokoyama, *Bull. Chem. Soc. Jpn.* **2000**, *73*, 191–196; c) Y. Yokoyama, *Chem. Rev.* **2000**, *100*, 1717–1740.
[19] M. Suarez, G. B. Schuster, *J. Am. Chem. Soc.* **1995**, *117*, 6732–6738.
[20] Y. Kim, M. Frigoli, N. Vanthuyne, N. Tamaoki, *Chem. Commun.* **2017**, *53*, 200–203.
[21] a) S.-Y. Lu, L.-C. Chien, *Appl. Phys. Lett.* **2007**, *91*, 131119; b) T. Yoshioka, T. Ogata, T. Nonaka, M. Moritsugu, S. -N. Kim, S. Kurihara, *Adv. Mater.* **2005**, *17*, 1226–1229; c) J. Li, H. K. Bisoyi, J. Tian, J. Guo, Q. Li, *Adv. Mater.* **2019**, *31*, 1807751.
[22] a) N. Y. Ha, Y. Ohtsuka, S. M. Jeong, S. Nishimura, G. Suzaki, Y. Takanishi, K. Ishikawa, H. Takezoe, *Nat. Mater.* **2008**, *7*, 43–47; b) M. Mitov, *Adv. Mater.* **2012**, *24*, 6260–6276
[23] a) S. Furumi, N. Tamaoki, *Adv. Mater.* **2010**, *22*, 886–891; b) Z. Zheng, B. Liu, L. Zhou, W. Wang, W. Hub, D. Shen, *J. Mater. Chem. C* **2015**, *3*, 2462–2470.
[24] a) A. Ryabchun, A. Bobrovsky, J. Stumpe, V. Shibaev, *Adv. Opt. Mater.* **2015**, *3*, 1273; b) A. Ryabchun, A. Bobrovsky, *Adv. Opt. Mater.* **2018**, *6*, 1800335; c) R. S. Zola, H. K. Bisoyi, H. Wang, A. M. Urbas, T. J. Bunning, Q. Li, *Adv. Mater.* **2019**, *31*, 1806172.
[25] a) R. Thomas, Y. Yoshida, T. Akasaka, N. Tamaoki, *Chem. Eur. J.* **2012**, *18*, 12337–12348; b) A. Kausar, H. Nagano, Y. Kuwahara, T. Ogata, S. Kurihara, *Chem. Eur. J.* **2011**, *17*, 508–515; c) R. Eelkema, M. M. Pollard, J. Vicario, N. Katsonis, B. S. Ramon, C. W. M. Bastiaansen, D. J. Broer, B. L. Feringa, *Nature*, **2006**, *440*, 123–123; d) R. Eelkema, M. M. Pollard, N. Katsonis, J. Vicario, D. J. Broer, B. L. Feringa, *J. Am. Chem. Soc.* **2006**, *128*, 14397–14407; e) A. Bosco, M. G. M. Jongejan, R. Eelkema, N. Katsonis, E. Lacaze, A. Ferrarini, B. L. Feringa, *J. Am. Chem. Soc.* **2008**, *130*, 14615–14624; f) L. Wang, Q. Li, *Chem. Soc. Rev.* **2018**, *47*, 1044–1097.
[26] Y. Kim, N. Tamaoki, *ACS Appl. Mater. Interfaces*, **2016**, *8*, 4918–4926.
[27] Md. Z. Alam, T. Yoshioka, T. Ogata, T. Nonaka, S. Kurihara, *Chem. Eur. J.* **2007**, *13*, 2641–2647.
[28] M. Goh, K. Akagi, *Liq. Cryst.* **2008**, *35*, 953–965.
[29] S. Pieraccini, S. Masiero, G. P. Spada, G. Gottarelli, *Chem. Commun.* **2003**, 598–599.
[30] a) S. Pieraccini, G. Gottarelli, R. Labruto, S. Masiero, O. Pandoli, G. P. Spada, *Chem. Eur. J.* **2004**, *10*, 5632–5639; b) Q. Li, L. Green, N. Venkataraman, I. Shiyanovskaya, A. Khan, A. Urbas, J. W. Doane, *J. Am. Chem. Soc.* **2007**, *129*, 12908–12909; c) J. Ma, Y. Li, T. White, A. Urbas, Q. Li, *Chem. Commun.* **2010**, *46*, 3463–3465.
[31] Y. Li, M. Wang, T. J. White, T. J. Bunning, Q. Li, *Angew. Chem. Int. Ed.* **2013**, *52*, 8925–8929; *Angew. Chem.* **2013**, *125*, 9093–9097.
[32] a) D. Fu, J. Li, J. Wei, J. Guo, *Soft Matter,* **2015**, *11*, 3034–3045; b) H. Wang, H. Krishna Bisoyi, L. Wang, A. M. Urbas, T. J. Bunning, Q. Li, *Angew. Chem. Int. Ed.* **2018**, *57*, 1627–1631; *Angew. Chem.* **2018**, *130*, 1643–1647.
[33] Y. Wang, A. Urbas, Q. Li, *J. Am. Chem. Soc.* **2012**, *134*, 3342–3345.
[34] a) L. Qin, W. Gu, J. Wei, Y. Yu, *Adv. Mater.* **2017**, *30*, 1704941; b) H. Huang, T. Orlova, B. Matt, N. Katsonis, *Macromol. Rapid Commun.* **2018**, *39*, 1700387.
[35] a) M. Mathews, R. S. Zola, S. Hurley, D.-K. Yang, T. J. White, T. J. Bunning, Q. Li, *J. Am. Chem. Soc.* **2010**, *132*, 18361–18366; b) H. Nishikawa, D. Mochizuki, H. Higuchi, Y. Okumura, H. Kikuchi, *ChemistryOpen* **2017**, *6*, 710–720; c) H. B. Lu, X. Y. Xie, J. Xing, C. Xu, Z. Q. Wu, G. B. Zhang, G. Q. Lv, L. Z. Qiu, *Opt. Mater. Express* **2016**, *6*, 3145–3158
[36] a) M. Mathews, N. Tamaoki, *J. Am. Chem. Soc.* **2008**, *130*, 11409–11416; b) M. C. Basheer, Y. Oka, M. Mathews, N. Tamaoki, *Chem. Eur. J.* **2010**, *16*, 3489–3496; c) N. Tamaoki, M. Wada, *J. Am. Chem. Soc.* **2006**, *128*, 6284–6285; d) Y. Kim, N. Tamaoki, *J. Mater. Chem. C.* **2014**, *2*, 9258–9264; e) M. Mathews, N. Tamaoki, *Chem. Commun.* **2009**, 3609–3611.
[37] K. S. Burnham, G. B. Schuster, *J. Am. Chem. Soc.* **1999**, *121*,10245–10246.
[38] a) S. N. Yarmolenko, L. A. Kutulya, V. V. Vashchenko, L. V. Chepeleva, *Liq. Cryst.* **1994**, *16*, 877–882; b) I. Gvozdovskyy, O. Yaroshchuk, M. Serbina, R. Yamaguchi, *Opt. Express* **2012**, *20*, 3499–3508.
[39] a) H. Qian, S. Pramanik, I. Aprahamian, *J. Am. Chem. Soc.* **2017**, *139*, 9140–9143; b) M. J. Moran, M. Magrini, D. M. Walba, I. Aprahamian, *J. Am. Chem. Soc.* **2018** *140*, 13623–13627.
[40] a) C. Denekamp, B. L. Feringa, *Adv. Mater.* **1998**, *10*, 1080–1082; b) T. Yamaguchi, H. Nakazumi, K. Uchida, M. Irie, *Chem. Lett.* **1999**, 653–654; c) T. Yamaguchi, T. Inagawa, H. Nakazumi, S. Irie, M. Irie, *Chem. Mater.* **2000**, *12*, 869–871; d) T. Yamaguchi, T. Inagawa, H. Nakazumi, S. Irie, M. Irie, *J. Mater. Chem.* **2001**, *11*, 2453–2458; e) T. van Leeuwen, T. C. Pijper, J. Areephong, B. L. Feringa, W. R. Browne, N. Katsonis, *J. Mater. Chem.* **2011**, *21*, 3142–3146.
[41] a) Y. Li, Q. Li, *Org. Lett.* **2012**, *14*, 4362–4365; b) Y. Li, M. Wang, H. Wang, A. Urbas, Q. Li, *Chem. Eur. J.* **2014**, *20*, 16286–16292; c) Y. Li, A. Urbas, Q. Li, *J. Am. Chem. Soc.* **2012**, *134*, 9573–9576; d) Y. Li, C. Xue, M. Wang, A. Urbas, Q. Li, *Angew. Chem. Int. Ed.* **2013**, *52*, 13703–13707; *Angew. Chem.* **2013**, *125*, 13948–13952; e) Y. Li, A. Urbas, Q. Li, *J. Org. Chem.* **2011**, *76*, 7148–7156; f) L. Wang, H. Dong, Y. Li, R. Liu, Y.-Y. Wang, H. K. Bisoyi, L.-D. Sun, C.-H. Yan, Q. Li, *Adv. Mater.* **2015**, *27*, 2065–2069.
[42] a) H. Hayasaka, T. Miyashita, M. Nakayama, K. Kuwada, K. Akagi, *J. Am. Chem. Soc.* **2012**, *134*, 3758–3765; b) Y. Li, M. Wang, A. Urbas, Q. Li, *J. Mater. Chem. C* **2013**, *1*, 3917–3923.
[43] a) Z. Zheng, Y. Li, H. K. Bisoyi, L. Wang, T. J. Bunning, Q. Li, *Nature*, **2016**, *531*, 352–356; b) Z. Zheng, R. S. Zola, H. K. Bisoyi, L. Wang, Y. Li, T. J. Bunning, Q. Li, *Adv. Mater.* **2017**, *29*, 1701903.
[44] a) S. Z. Janicki, G. B. Schuster, *J. Am. Chem. Soc.* **1995**, *117*, 8524–8527; b) T. J. White, A. D. Zhao, S. A. Cazzell, T. J. Bunning, T. Kosa, L. Sukhomlinova, T. J. Smith, B. Taheri, *J. Mater. Chem.* **2012**, *22*, 5751–5757.
[45] a) A. Ferrarini, S. Pieraccini, S. Masiero, G. P. Spada, *Beilstein J. Org. Chem.* **2009**, *5*, 1; b) G. Gottarelli, G. Proni, G. P. Spada, D. Fabbri, S. Gladiali, C. Rosini, *J. Org. Chem.* **1996**, *61*, 2013–2019.
[46] a) M. Frigoli, F. Maurel, J. Berthet, S. Delbaere, J. Marrot, M. M. Oliveira, *Org. Lett.* **2012**, *14*, 4150–4153; b) M. Frigoli, J. Marrot, P. L. Gentili, D. Jacquemin, M. Vagnini, D. Pannacci, F. Ortica, *ChemPhysChem* **2015**, *16*, 2447–2458.
[47] a) B. L. Feringa, N. P. M. Huck, H. A. van Doren, *J. Am. Chem. Soc.* **1995**, *117*, 9929–9930; b) N. Koumura, R. W. J. Zijlstra, R. A. van Delden, N. Harada, B. L. Feringa, *Nature*, **1999**, *401*, 152–155; c) T. C. Pijper, D. Pijper, M. M. Pollard, F. Dumur, S. G. Davey, A. Meetsma, B. L. Feringa, *J. Org. Chem.* **2010**, *75*, 825–838; d) J. C. M. Kistemaker, P. Stacko, D. Roke, A. T. Wolters, G. H.e Heideman, M.-C. Chang, P. van der Meulen, J. Visser, E. Otten, B. L. Feringa, *J. Am. Chem. Soc.* **2017**, *139*, 9650–9661; e) R. A. van Delden, N. Koumura, N. Harada, B. L. Feringa, *Proc. Natl. Acad. Sci. U.S.A.* **2002**, *99*, 4945–4949.
[48] a) T. J. White, S. A. Cazella, A. S. Freer, D. Yang, L. Sukhomlinova, L. Su, T. Kosa, B. Taheri, T. J. Bunning, *Adv. Mater.* **2011**, *23*, 1389–1392; b) S. J. Aßhoff, S. Iamsaard, A. Bosco, J. J. L. M. Cornelissen, B. L. Feringa, N. Katsonis, *Chem. Commun.* **2013**, *49*, 4256–4258.
[49] a) T. Orlova, F. Lancia, C. Loussert, S. Iamsaard, N. Katsonis, E. Brasselet, *Nature Nanotech.* **2018**, *13*, 304–308; b) P. Sleczkowski, Y. Zhou, S. Iamsaard, J. J. de Pablo, N. Katsonis, E. Lacaze *PNAS*, **2018**, *115*, 4334–4339.
[50] W.-C. Chen, P.-C. Lin, C.-H. Chen, C.-T. Chen, *Chem. Eur. J.* **2010**, *16*, 12822–12830.
[51] N. P. M. Huck, W. F. Jager, B. de Lange, B. L. Feringa, *Science*, **1996**, *273*, 1686–1688.

Manuscript received: February 20, 2019
Revised manuscript received: March 15, 2019
Version of record online: ■■, ■■■

© 2019 Wiley-VCH Verlag GmbH & Co. KGaA, Weinheim

REVIEWS

Around the twist: Recent advances in the design of photoisomerizable chiral dopants which can switch the helical orientation in cholesteric liquid crystals upon application of a light stimulus are reviewed. Such systems may find application in advanced optical and mechanical functions.

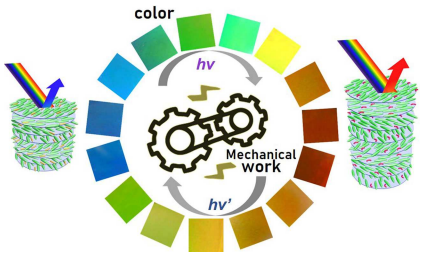

Dr. Y. Kim, Prof. N. Tamaoki**

1 – 21

Photoresponsive Chiral Dopants: Light-Driven Helicity Manipulation in Cholesteric Liquid Crystals for Optical and Mechanical Functions